Field-induced gap in Cu benzoate and other $S=\frac{1}{2}$ antiferromagnetic chains

Ian Affleck

*Department of Physics and Astronomy and Canadian Institute for Advanced Research, The University of British Columbia,
Vancouver, British Columbia, Canada V6T 1Z1*

Masaki Oshikawa

Department of Physics, Tokyo Institute of Technology, Oh-okayama, Meguro-ku, Tokyo 152-8551, Japan
(Received 12 February 1999)

Recent experiments on the $S=\frac{1}{2}$ antiferromagnetic chain compound, Cu benzoate, discovered an unexpected gap scaling as approximately the $\frac{2}{3}$ power of an applied magnetic field. A theory of this gap, based on an effective staggered field, orthogonal to the applied uniform field, resulting from a staggered gyromagnetic tensor and a Dzyaloshinskii-Moriya interaction, leading to a sine-Gordon quantum field theory, has been developed. Here we discuss many aspects of this subject in considerable detail, including a review of the $S=\frac{1}{2}$ chain in a uniform field, a spin-wave theory analysis of the uniform plus staggered field problem, exact amplitudes for the scaling of gap, staggered susceptibility and staggered magnetization with field or temperature, intensities of soliton and breather peaks in the structure function, and field and temperature dependence of the total susceptibility. [S0163-1829(99)03226-9]

I. INTRODUCTION

The effect of a magnetic field on an $S=\frac{1}{2}$ antiferromagnetic chain has been extensively investigated theoretically over many years. The Hamiltonian is written

$$\hat{H}=\sum_j \ [J\vec{S}_j\cdot\vec{S}_{j+1}-g\mu_B HS_j^z]. \qquad (1.1)$$

An important conclusion was that the ground state remains gapless right up to the saturation field. The low-energy excitations can be described by bosonization which predicts gapless excitations at wave vectors 0 and π and also at the incommensurate wave vectors

$$k_1=\pm 2\pi m(H), \quad k_2=\pi\pm 2\pi m(H), \qquad (1.2)$$

where $m(H)$ is the magnetization per site, $m\equiv\langle S_i^z\rangle$. The first detailed experimental study of such systems at large fields with $g\mu_B H$ of $O(J)$ were only performed very recently,[1] on Cu benzoate. This material has a relatively small exchange energy, $J\approx 1.57$ meV so that $g\mu_B H/J\approx 0.52$ for a field of 7 T. While these experiments verified, in detail, the expected field-dependent shift of the wave-vector at which a gap minimum occurs, they also discovered an unexpected result. A non-zero gap appeared which seemed to scale as approximately $H^{2/3}$, with strong dependence on the field orientation. Dender *et al.*[1] suggested that this gap might arise from the staggered g (gyromagnetic) tensor, associated with the low symmetry of the crystal structure and the presence of two crystallographically inequivalent Cu sites on each chain. Thus the last term in Eq. (1.1) must be replaced by

$$\hat{H}_H=-\mu_B\sum_{j,a,b}H^a[g_{ab}^u+(-1)^jg_{ab}^s]S_j^b. \qquad (1.3)$$

This results in the presence of an effective staggered field, $g^s\vec{H}$, upon the application of a uniform field. Such a staggered field, which couples directly to the Néel order parameter, is expected to produce an ordered antiferromagnetic moment and a gap which scale with field.

This idea was developed in detail in Ref. 2 where it was found that a staggered Dzyaloshinskii-Moriya[3,4] (DM) interaction also contributes a roughly equal amount to this effective staggered field. This corresponds to an additional term in the Hamiltonian:

$$\hat{H}_{DM}=\sum_j \ (-1)^j\vec{D}\cdot(\vec{S}_{j-1}\times\vec{S}_j). \qquad (1.4)$$

It was found that several aspects of the experiments could be explained in detail by this model. These include the field orientation dependence of the gap and its scaling with field magnitude. Much of this work used the bosonization technique which maps the problem onto the sine-Gordon model, for which various exact results are available. The excitations observed in neutron scattering were identified with the soliton, antisoliton, and ''breather'' (soliton-antisoliton bound-state) spectrum of the sine-Gordon model. Additional results, further supporting this approach, were obtained by Essler and Tsvelik.[5] As shown below, the effective staggered field is essentially perpendicular to the uniform field. We note that the case of a staggered field parallel to the uniform field maps into a related sine-Gordon model and was analyzed in Ref. 6. The purpose of this paper is to provide more details and some extensions of the results in Ref. 2. While Cu benzoate is the only example of such a system that we discuss in the present paper, it should be possible to apply our theory to other quasi-one dimensional system with similar crystallographic structure.

In the absence of a staggered field, the critical behavior of the antiferromagnet is determined by three field dependent quantities: the magnetization, $m(H)$ [which determines the soft wave vectors via Eq. (1.2)], the spin-wave velocity, $v(H)$ and the boson compactification radius (which deter-

mines the critical exponents), $R(H)$. All three of these quantities can be determined very accurately by numerical solution of Bethe ansatz equations. Furthermore, we derive an exact relationship between these three functions using field theory arguments. We also derive the logarithmic dependence of R on H, as $H \rightarrow 0$, from the existence of a marginally irrelevant operator, using the renormalization group.

We determine the scaling of gap with staggered field, order parameter with field, and susceptibility with temperature. The calculations are done including logarithmic corrections which arise from a marginally irrelevant operator and take into account both uniform and staggered fields. Furthermore, the exact amplitudes of the scaling functions are determined using a recent result of Lukyanov and Zamalodchikov.[7] (After this calculation was finished we received the report[8] which gives the same result for the gap, without a discussion of logarithmic corrections.) We also give some further discussion of the structure factors $S^a(q,\omega)$, measured in neutron scattering. We discuss a hidden SU(2) symmetry of the model. We prove that the longitudinal structure factor (for ''a'' corresponding to the uniform field direction) gets contributions from only the soliton and antisoliton intermediate states, in agreement with experiment. On the other hand, the transverse structure function gets contributions only from the breathers. Using the approximate $SU(2)$ symmetry, we discuss the relative intensity of the various single-particle peaks in the neutron-scattering cross section, taking into account the polarization dependent factors which arise from Fourier transforming the dipole interaction between neutrons and spins which were omitted in Ref. 5. A comparison is made with experimental results. In particular, the problem of determining a consistent value for the DM vector, $\vec{D}$ is discussed. The susceptibility of the sine-Gordon model is calculated, using the integrability of the model, giving essentially the field and temperature dependence of the staggered susceptibility of the antiferromagnet.

In Sec. II we discuss the DM interaction and the mapping of the system into a Heisenberg model with orthogonal uniform and staggered fields. In Sec. III we treat this problem using conventional spin-wave theory. In Sec. IV we discuss bosonization in the presence of a uniform magnetic field. In Sec. V we extend the bosonization approach to the case with staggered field and analyze the induced gap. In Sec. VI we discuss structure factors and compare with the observed neutron scattering cross section. In Sec. VII we present estimates of the DM interaction based on several experimental results. In Sec. VIII we discuss the magnetization and susceptibility.

II. EFFECTIVE HAMILTONIAN

The crystal structure of Cu benzoate is shown in Fig. 1 and Fig. 2. The chain direction is the c axis. Note that each Cu atom is surrounded by six ligands with a local symmetry which is almost tetragonal. However the principal axes for this tetragonal symmetry alternate along the chain, with the two inequivalent c axes being rotated by $10°$ relative to each other. These corresponding c axes are labeled I and II in Fig. 3. The b axes are the same for both Cu sites. Neither of these sets of principal axes correspond to the crystal axes. It is expected that the principal axes for the gyromagnetic tensor
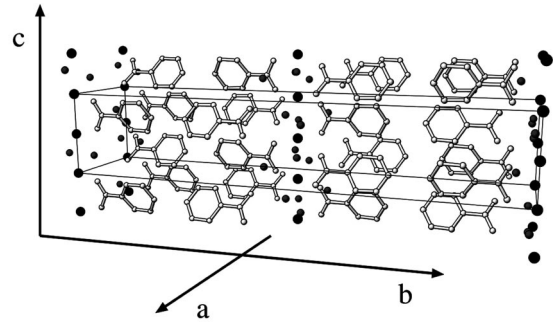

FIG. 1. Crystal structure of Cu benzoate. Filled circles are Cu^{2+} ions, connected atoms are benzoate group, and grey circles represent H_2O molecules. Unit cell is shown as a frame, and arrows indicate crystal axes part of the figure.

will also alternate, corresponding to the local tetragonal axes around each Cu ion. The principal axis for the anisotropic exchange interaction is expected to be the c' axes, the perpendicular bisector of I and II axes. On the other hand, the principal axis for the dipole interaction, which is of roughly the same order of magnitude is essentially the c axis. Combining these two types of contributions to the nearest neighbor spin-spin interaction, gives a principal axis which roughly bisects c' and c, and is denoted c'' in Fig. 4. It is convenient to refer the g tensor to this a''-b-c'' coordinate
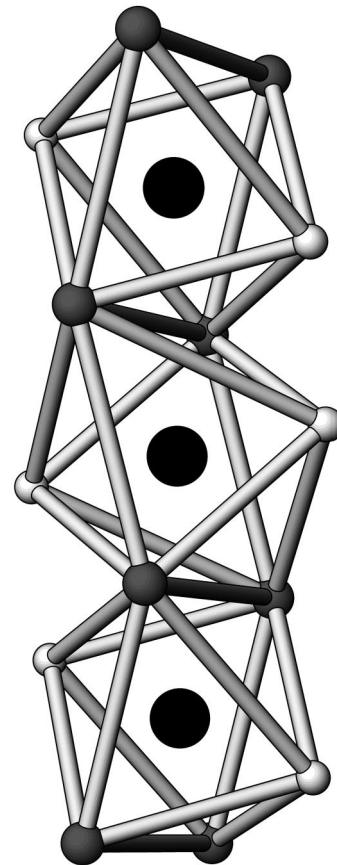

FIG. 2. Enlargement of crystal structure near a Cu (black spheres) chain with O atoms of H_2O (dark spheres) and those of benzoate groups (light spheres). Note that the oxygen octahedra have two different orientations on staggered Cu atoms.
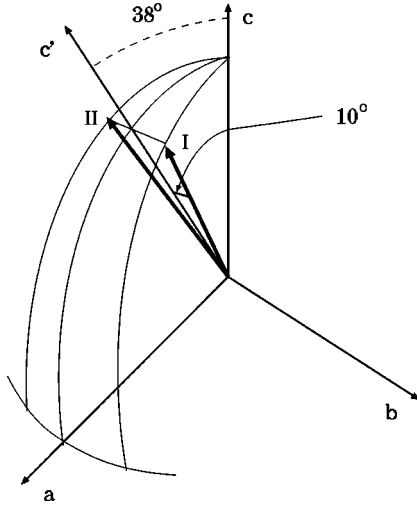
FIG. 3. Local magnetic principal axes of inequivalent Cu sites (I and II). The principal axes of the average g tensors are denoted as a', b, and c'.

system. From electron spin resonance (ESR) measurements,[9] it takes the form

$$
g = \begin{pmatrix} 2.115 & \pm 0.0190 & 0.0906 \\ \pm 0.0190 & 2.059 & \pm 0.0495 \\ 0.0906 & \pm 0.0495 & 2.316 \end{pmatrix} \equiv g^u \pm g^s,
$$

(2.1)

with the $\pm$ referring to the two inequivalent Cu sites. g^u and g^s are the uniform and staggered parts of the g tensor. This staggered g tensor produces an effective staggered field, $\pm g^s \vec{H}$, while the uniform g tensor produces an effective uniform field $g^u \vec{H}$. In the special cases where the applied field is along the b axis or in the $a''c''$ plane the effective staggered field is perpendicular to the applied field and also to the effective uniform field. For general directions of the applied field they are almost perpendicular (to within a few %).
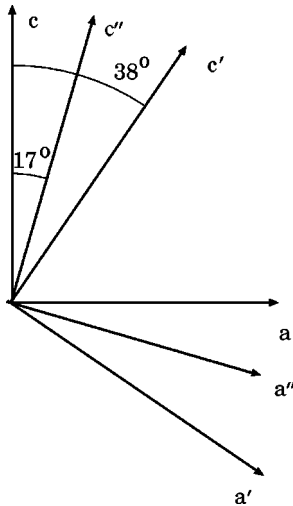

FIG. 4. Local principal axes of combined magnetic interactions a'' and c'', shown in ac plane.

As discussed by Dzyaloshinskii[3] and Moriya,[4] in magnetic crystals of low symmetry an additional antisymmetric exchange interaction occurs, the DM interaction

$$
\hat{H}_{DM} = \sum_j \vec{D}_j \cdot (\vec{S}_j \times \vec{S}_{j+1}).
$$

(2.2)

The possible values of the DM vector $\vec{D}_j$ can be limited by considering crystal symmetries of Cu benzoate. First, the compound is invariant under a translation along the c axis by two sites. This means the DM vectors are the same among the even (or odd) links, but even and odd DM vectors can be different. Secondly, there is a symmetry under rotation by angle π about an axis parallel to the b axis that passes through the midpoint of two neighboring sites (j and $j+1$), along the chains (c axis). As noticed by Moriya,[4] this implies the DM vector for the interaction between j and $j+1$ must be orthogonal to the b axis. This can be shown as follows: assume we have the DM interaction $\vec{D} \cdot (\vec{S}_j \times \vec{S}_{j+1})$. Now apply the rotation described above. It acts on the spin operators as $S_k^{a,c} \to -S_{2j+1-k}^{a,c}$ and $S_k^b \to S_{2j+1-k}^b$. Thus, for the b component of $\vec{D}$, the DM interaction would be inverted while it is unchanged for the a,c component of $\vec{D}$ implying that $D^b = 0$. Finally, the crystal structure is invariant under the combined operation of one site translation along the chain (c) direction *and* reflection in the ac plane. Considering the fact that the spin vector $\vec{S}_j$ is an axial vector, the operation acts as $S_k^{a,c} \to -S_{k+1}^{a,c}$ and $S_k^b \to S_{k+1}^b$. Since the DM vector is orthogonal to the b axis (and thus one factor of S^b always appears in the outer product), the DM interaction term is inverted by the combined operation: $\vec{D} \cdot (\vec{S}_j \times \vec{S}_{j+1}) \to -\vec{D} \cdot (\vec{S}_{j+1} \times \vec{S}_{j+2})$. Thus, the DM vector is alternating as in Eq. (1.4). There are apparently no other restrictions that can be placed on the DM vector using symmetry alone. By considering a tight-binding model for the exchange interactions it was estimated[4] that D/J is of $O(\delta g/g)$ where δg is the deviation of g from twice the identity matrix.

Apart from the antisymmetric DM interaction, the remaining exchange anisotropy is believed to be quite negligible (about 1% of J) and we will henceforth ignore it. Taking $\vec{D} \propto \hat{z}$, we may write the Hamiltonian

$$
\hat{H} = \frac{1}{2} \sum_j [\mathcal{J} S_{2j-1}^+ S_{2j}^- + \mathcal{J}^* S_{2j}^+ S_{2j+1}^- + (\text{H.c.})]
$$

$$
+ J \sum_j [S_{2j-1}^z S_{2j}^z + S_{2j}^z S_{2j+1}^z],
$$

(2.3)

where $\mathcal{J} \equiv J + iD$. Performing a rotation[10] of the spins by an angle $\pm \alpha/2$:

$$
S_{2j}^+ \to S_{2j}^+ e^{i\alpha/2}, \quad S_{2j+1}^+ \to S_{2j+1}^+ e^{-i\alpha/2},
$$

(2.4)

where

$$
\tan \alpha = D/J,
$$

(2.5)

the Hamiltonian is transformed to the standard xxz model:

$$
\hat{H} = \sum_j \left[J S_j^z S_{j+1}^z + \frac{|\mathcal{J}|}{2} (S_j^+ S_{j+1}^- + \text{H.c.}) \right].
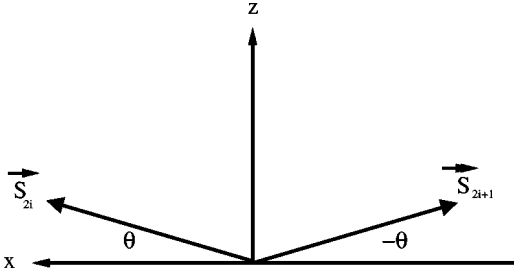$$

(2.6)

FIG. 5. Classical spin configuration.

With some assumptions this anisotropic exchange may cancel the preexisting one. In any event, it is small and we will ignore it.

　　Now consider an external magnetic field, approximating the g tensor as two times the identity matrix. The spin redefinition of Eq. (2.4) introduces an effective staggered field. For example, for a uniform field in the x direction

$$-H\sum_j S_j^x \rightarrow -H\sum_j \left[\cos\frac{\alpha}{2}S_j^x + (-1)^j \sin\frac{\alpha}{2}S_j^y\right]. \quad (2.7)$$

Combining the actual form of the g tensor with the DM interaction, we can obtain effective uniform and staggered fields corresponding to an arbitrary applied one. Writing the rotation matrices by $\pm\alpha/2$ around $\vec{D}$ as

$$\mathcal{R}_{\vec{D}}(\pm\alpha/2)\equiv\mathcal{R}^u \pm \mathcal{R}^s, \quad (2.8)$$

the effective uniform and staggered fields are defined by

$$\vec{H}^u \equiv [\mathcal{R}^u g^u + \mathcal{R}^s g^s]\vec{H},$$

$$\vec{H}^s \equiv [\mathcal{R}^s g^u + \mathcal{R}^u g^s]\vec{H}. \quad (2.9)$$

In general, $\vec{H}^s$ is nearly orthogonal to $\vec{H}^u$. For small g^s and D/J, the staggered field can be approximated as

$$\vec{H}^s \sim g^s\vec{H} + \frac{1}{2J}\vec{D}\times g^u\vec{H}, \quad (2.10)$$

namely the sum of two contributions.

　　Henceforth, since we are ignoring the small residual exchange anisotropy and assuming that $\vec{H}^u\perp\vec{H}^s$, we will take $\vec{H}^u$ to be in the z direction and $\vec{H}^s$ to be in the x direction and refer to them as simply H and h, respectively. Also setting $2\mu_B=1$ we arrive at the simple effective Hamiltonian:

$$\hat{H}_{\text{eff}}=\sum_i [J\vec{S}_i\cdot\vec{S}_{i+1} - HS_i^z - h(-1)^iS_i^x], \quad (2.11)$$

with $h\ll H$. (Note that we have switched the directions of the uniform and applied fields relative to our earlier paper[2] which, unfortunately, contained some inconsistencies of notation.)

III. SPIN-WAVE THEORY

　　In this section we summarize the results of spin-wave theory (leading order $1/S$ expansion) for the effective Hamiltonian of Eq. (2.11). (As far as we know, spin-wave theory results for this problem were first published in Ref. 11.) Al-

though this misses certain features caused by quantum fluctuations in one dimension, it is still quite instructive.

　　The classical ground state is a canted antiferromagnetic structure, shown in Fig. 5. The spins on both sublattices lie in the xz plane canted towards the z axis by an angle θ from the $\pm x$ axis. The classical energy of this state is

$$E(\theta)/L = -JS^2\cos 2\theta - hS\cos\theta - HS\sin\theta. \quad (3.1)$$

This is minimized for θ the solution of

$$4JS^2\sin\theta\cos\theta + hS\sin\theta - HS\cos\theta = 0. \quad (3.2)$$

For $h=0$, the solution is

$$\sin\theta = H/4JS. \quad (3.3)$$

In order to do a systematic $1/S$ expansion, it is convenient to regard H and h as being of $O(S)$. We assume that H is less than the saturation field, $4JS$. The leading order spin-wave expansion for a spin pointing in the x direction is

$$\vec{S}_j^0 \approx \left[S - a_j^\dagger a_j, \sqrt{\frac{S}{2}}(a_j^\dagger + a_j), i\sqrt{\frac{S}{2}}(a_j^\dagger - a_i)\right]. \quad (3.4)$$

Here a_j is a boson annihilation operator. To consider small fluctuations about the canted structure we simply write

$$\vec{S}_{2i} \approx \mathcal{R}_y\vec{S}_{2i}^0,$$

$$\vec{S}_{2i+1} \approx \mathcal{R}_z\mathcal{R}_y\vec{S}_{2i+1}^0, \quad (3.5)$$

where $\mathcal{R}_y$ is a rotation about the y axis by $-\theta$:

$$\mathcal{R}_y \equiv \begin{pmatrix} \cos\theta & 0 & -\sin\theta \\ 0 & 1 & 0 \\ \sin\theta & 0 & \cos\theta \end{pmatrix}, \quad (3.6)$$

and $\mathcal{R}_z$ is a rotation by π about the z axis:

$$\mathcal{R}_z \equiv \begin{pmatrix} -1 & 0 & 0 \\ 0 & -1 & 0 \\ 0 & 0 & 1 \end{pmatrix}. \quad (3.7)$$

Using the facts that

$$\mathcal{R}_z^T = \mathcal{R}_z,$$

$$(\mathcal{R}_z\mathcal{R}_y)_{3i} = (\mathcal{R}_y)_{3i},$$

$$(\mathcal{R}_z\mathcal{R}_y)_{1i} = -(\mathcal{R}_y)_{1i}, \quad (3.8)$$

the Hamiltonian may be written in a manifestly translationally invariant way:

$$\hat{H}=\sum_j [J\vec{S}_j^0\cdot\mathcal{R}_y^T\mathcal{R}_z\mathcal{R}_y\vec{S}_{j+1}^0 - H(\mathcal{R}_y\vec{S}_j^0)_z - h(\mathcal{R}_y\vec{S}_j^0)_x]. \quad (3.9)$$

It is the translational invariance of Eq. (3.9) which motivated the somewhat peculiar looking choice of transformation matrices in Eq. (3.5). Substituting Eq. (3.5) into the Hamiltonian of Eq. (3.9), we find that the term of $O(S^2)$ is a c number and the term of $O(S^{3/2})$ vanishes. The term of $O(S)$ is

$$\hat{H} \approx \sum_j \; [(2JS \cos 2\theta + H \sin \theta + h \cos \theta)a_j^\dagger a_j$$

$$+ (JS/2)(\cos 2\theta - 1)(a_j^\dagger a_{j+1} + a_{j+1}^\dagger a_j)$$

$$+ (JS/2)(\cos 2\theta + 1)(a_j^\dagger a_{j+1}^\dagger + a_j a_{j+1})]. \quad (3.10)$$

Fourier transforming and performing a Bogoliubov transformation that mixes a_k with $a_{-k}^\dagger$, we obtain a single band of spin waves in the paramagnetic Brillouin zone, $-\pi < k < \pi$ with dispersion relation

$$E(k) = \{[2JS \cos 2\theta + H \sin \theta + h \cos \theta$$

$$- JS(1 - \cos 2\theta)\cos k]^2$$

$$- [JS(1 + \cos 2\theta)\cos k]^2\}^{1/2}. \quad (3.11)$$

The above transformation has allowed us to obtain a single band in the paramagnetic Brillouin zone. We may equivalently fold the dispersion relation into the antiferromagnetic Brillouin zone, $-\pi/2 < k < \pi/2$. This gives us two branches of spin waves with dispersion relations

$$E_\pm(k) = \{[2JS \cos 2\theta + H \sin \theta + h \cos \theta$$

$$\pm JS(1 - \cos 2\theta)\cos k]^2$$

$$- [JS(1 + \cos 2\theta)\cos k]^2\}^{1/2}. \quad (3.12)$$

While this is a fairly simple and explicit formula for the energies in terms of θ, it must be borne in mind that θ is determined in terms of J, H, and h by Eq. (3.2). In the special case $h = 0$, using Eq. (3.3), we obtain

$$E_\pm(k) = 2JS \left[\sin^2 k + 2 \left(\frac{H}{4JS} \right)^2 (\cos^2 k \pm \cos k) \right]^{1/2}. \quad (3.13)$$

Note that at $k = 0$, or equivalently $k = \pi$,

$$E_- = 0,$$

$$E_+ = H. \quad (3.14)$$

The E_- mode is the Goldstone mode corresponding to a uniform precession about the z axis. A nonzero h gives this mode a gap, pinning the spins along the x axis. We may calculate this gap, to lowest order in h using, from Eq. (3.2), $\theta = \sin^{-1}(H/4JS) + \delta\theta$ where

$$\delta\theta \approx -\frac{Hh}{16J^2S^2 - H^2}. \quad (3.15)$$

To linear order the gap is given by

$$\Delta^2 \approx \frac{\partial E_-^2}{\partial \theta} \delta\theta + \frac{\partial E_-^2}{\partial h} h. \quad (3.16)$$

Thus

$$\Delta \approx \sqrt{4JSh[1 + (H^2/8J^2S^2)]}[1 - (H/4JS)^2]^{1/4} + O(h^{3/2}). \quad (3.17)$$

Note that Δ is a singular function of the staggered field, exhibiting a mean field exponent of 1/2. On the other hand, it depends only weakly on the uniform field, being almost in-

dependent of H up to H of $O(JS)$. While this mean field exponent changes when one-dimensional quantum fluctuations are taken into account, it is reasonable to expect this weak dependence on H to remain true. The upper mode, $E_+(0)$ depends strongly on H but only weakly on h. For $h \ll H$, $E_+(0) \approx H$.

IV. BOSONIZATION FOR 0 STAGGERED FIELD

In the one-dimensional case, an exact picture of the low-energy behavior can be obtained using bosonization and RG arguments. Here we summarize the results for the case of a uniform field, but no staggered field.

We begin with the case where the uniform field also vanishes. The low energy degrees of freedom of the quantum spin variables can be represented in terms of a free boson with Lagrangian density:

$$\mathcal{L} = \frac{1}{2}[(\partial_t\phi)^2 - v_s^2(\partial_x\phi)^2]. \quad (4.1)$$

(Here v_s is the spin-wave velocity which we will generally set equal to 1.) The boson field, ϕ can be separated into left and right moving terms:

$$\phi(t,x) = \phi_L(t+x) + \phi_R(t-x). \quad (4.2)$$

Their difference defines the dual field:

$$\tilde{\phi} = \phi_L - \phi_R. \quad (4.3)$$

For $H = 0$ there are low energy degrees of freedom at wave vectors 0 and π. The spin operators can be approximated as

$$S_j^z \approx \frac{1}{2\pi R} \frac{\partial\phi}{\partial x} + \text{const}(-1)^j \cos\frac{\phi}{R},$$

$$S_j^- \approx e^{i2\pi R\tilde{\phi}} \left[\text{const} \, \cos\frac{\phi}{R} + C(-1)^j \right]. \quad (4.4)$$

(The first constant above is universal. The next three are not, but C has been recently determined using the integrability of the model[6,12] and will be discussed in the next section.)

For the $H = 0$ Heisenberg model, $R = 1/\sqrt{2\pi}$. For the xxz model R (and C) vary with the anisotropy parameter. Writing the Hamiltonian

$$H = J\sum_j \; [S_j^x S_{j+1}^x + S_j^y S_{j+1}^y + \delta S_j^z S_{j+1}^z], \quad (4.5)$$

exact Bethe ansatz results determine

$$2\pi R^2 = 1 - \frac{\cos^{-1}\delta}{\pi}. \quad (4.6)$$

R varies between $1/\sqrt{2\pi}$ and 0 along the xxz critical line, $-1 < \delta < 1$.

In order to understand the vicinity of the isotropic antiferromagnetic point, $\delta = 1$, it is convenient to use non-Abelian bosonization:

$$\vec{S}_j \approx (\vec{J}_L + \vec{J}_R) + \text{const}(-1)^j \, \text{tr}(\vec{\sigma}g). \quad (4.7)$$
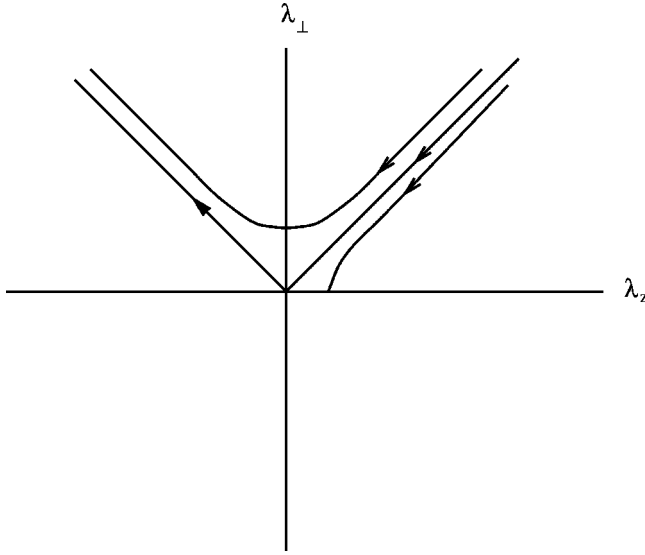
FIG. 6. The Kosterlitz-Thouless RG flows of Eq. (4.10).

Here g is the SU(2) matrix field of the Wess-Zumino-Witten, $k=1$ nonlinear σ model (WZW model). $\vec{J}_L$ and $\vec{J}_R$ are the left and right moving conserved currents associated with the SU(2) symmetry of the spin chain. By comparing Eqs. (4.4) and (4.7) we may read off the correspondences between the WZW fields and the free boson fields. These are

$$J_L^z = \frac{1}{\sqrt{8\pi}}\partial_-\phi, \quad J_R^z = -\frac{1}{\sqrt{8\pi}}\partial_+\phi,$$

$$J_L^- \propto e^{i\sqrt{8\pi}\phi_L}, \quad J_R^- \propto e^{-i\sqrt{8\pi}\phi_R},$$

$$g \propto \begin{pmatrix} e^{i\sqrt{2\pi}\phi} & e^{-i\sqrt{2\pi}\tilde{\phi}} \\ -e^{i\sqrt{2\pi}\tilde{\phi}} & e^{-i\sqrt{2\pi}\phi} \end{pmatrix}. \tag{4.8}$$

Here $\partial_\pm \equiv \partial_t \pm \partial_x$.

The bosonized spin-chain Lagrangian contains, in addition to the free boson Lagrangian, interaction terms

$$\mathcal{L}_{\text{int}} = \frac{8\pi^2}{\sqrt{3}}[\lambda_z J_L^z J_R^z + \lambda_\perp (J_L^x J_R^x + J_L^y J_R^y)]. \tag{4.9}$$

For the isotropic Heisenberg model, $\lambda_z = \lambda_\perp = O(1)$. Including small anisotropy, $\lambda_z - \lambda_\perp \propto 1-\delta$. These obey the RG equations:

$$d\lambda_z/d\ln E = (4\pi/\sqrt{3})\lambda_\perp^2 + O(\lambda^3),$$

$$d\lambda_\perp/d\ln E = (4\pi/\sqrt{3})\lambda_z\lambda_\perp + O(\lambda^3). \tag{4.10}$$

The RG trajectories are hyperbolas as shown in Fig. 6. For $\lambda_z > \lambda_\perp$, they end at the λ_z axis, corresponding to the xxz critical line. For $\lambda_z < \lambda_\perp$ they lead towards strong coupling, corresponding to the easy axis ordered phase. Reverting to Abelian bosonization, we see that the fixed point Lagrangian contains the extra term

$$\frac{8\pi^2}{\sqrt{3}}\lambda_z(0)J_L^z J_R^z = -\frac{\pi}{\sqrt{3}}\lambda_z(0)[(\partial_t\phi)^2 - (\partial_x\phi)^2]. \tag{4.11}$$

Since this is proportional to the free Lagrangian, we can eliminate it by a rescaling of ϕ. This corresponds to a rescaling of the parameter, R, decreasing it by an amount of $O(\lambda_z(0)) = O(1-\delta)$ in agreement with the Bethe ansatz result of Eq. (4.6).

We now consider the Heisenberg model with a uniform external field (but no staggered field). The extra term in the Lagrangian becomes, upon bosonization,

$$\mathcal{L}_H = \frac{H}{\sqrt{2\pi}}\frac{\partial\phi}{\partial x}. \tag{4.12}$$

This term can be eliminated by a redefinition of the boson field:

$$\phi(t,x) \rightarrow \phi(t,x) + \frac{H}{\sqrt{2\pi}}x. \tag{4.13}$$

This leaves the free Lagrangian unchanged. However, it does effect the interaction term and the bosonization formulas. The interaction term is changed due to the shift of the $\pm$ components of the currents:

$$J_{L,R}^- \rightarrow J_{L,R}^- e^{\pm iHx},$$

$$J_{L,R}^+ \rightarrow J_{L,R}^+ e^{\mp iHx},$$

$$J_{L,R}^z \rightarrow J_{L,R}^z. \tag{4.14}$$

(Note that the phases add, rather than cancel in the interaction term $J_L^+ J_R^-$.) The effect of these phases on the RG equations can be determined from a consideration of the operator product expansion (OPE). One of the OPE's gets shifted while the other one does not:

$$J_L^+(x)J_L^-(x') \rightarrow e^{iH(x'-x)}\frac{J_L^z}{x-x'},$$

$$J_L^+(x)J_L^z(x') \rightarrow \frac{J_L^+}{x-x'}. \tag{4.15}$$

The one-loop RG equations can be conveniently derived using an ultraviolet cutoff on the distance between any pairs of insertions of the interaction Lagrangian in perturbation theory. (See, for example, Ref. 13.) As the position space ultraviolet cutoff is increased from a to a', we integrate over that range of separation of the two points, using the OPE. The net effect is that, when the cutoff is small compared to $1/H$ the phase factor in the OPE is nearly constant and can be ignored. However, when the cutoff is large compared to $1/H$, the phase factor produces rapid oscillations which tend to cancel out the term from the effective renormalization. Reverting to an energy cutoff, this means that the RG equations of Eq. (4.10) are essentially correct for $E \gg H$, but for $E \ll H$ the right hand side should be replaced by 0 in the first equation. That is, λ_z ceases renormalizing, at E of $O(H)$ whereas $\lambda_\perp$ continues to renormalize as before. Thus the RG trajectories are essentially two straight lines. For $E \gg H$ the couplings renormalize along the isotropic separatrix, $\lambda_z(E) = \lambda_\perp(E)$, but for $E \ll H$, λ_z is constant and $\lambda_\perp$ renormalizes to 0. (See Fig. 7.) Thus, in order to determine $\lambda_z(0)$ we
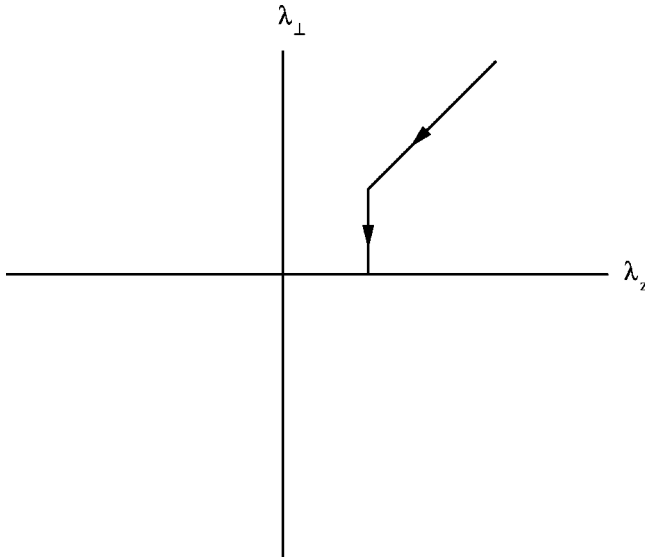
FIG. 7. The RG flows in the presence of a magnetic field. The turn occurs at an energy scale of O(H).

simply need to calculate $\lambda(H)$ using the isotropic RG equations of Eq. (4.10). For $H \ll J$, these give

$$\lambda(H) \approx \frac{\sqrt{3}}{4\pi \ln(J/H)}. \qquad (4.16)$$

This argument may seem rather naive and it certainly does not give the correct RG trajectory for E of $O(H)$. However, due to the weak, logarithmic, dependence of λ on E we expect that this argument gives the correct behavior of $\lambda_z(0)$ with H for $H \ll J$. This argument then determines the dependence of R on H for $H \ll J$:

$$2\pi R^2 = 1 - \frac{2\pi}{\sqrt{3}} \lambda_z(0) = 1 - \frac{1}{2\ln(J/H)}. \qquad (4.17)$$

Precisely this result was obtained from the Bethe ansatz[14] in the limit $H \ll J$. (See Fig. 8.) For larger values of H higher order terms in the RG equations would be needed and additional interactions would have to be considered, some of
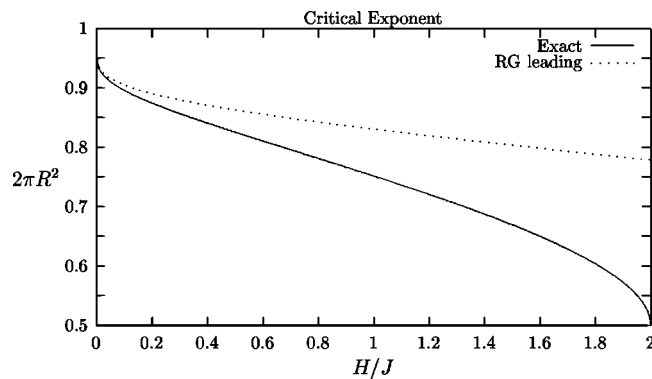

FIG. 8. Critical exponent $2\pi R^2$ as a function of the applied field H. Exact solution is compared with the leading terms $2\pi R^2 \sim 1 - 1/[2\log(H_0/H)]$ in the RG analysis. We show a good fit to the numerical solution of the Bethe ansatz integral equations with $H_0 = \sqrt{32\pi^3/e}$. This choice of H_0 is four times the value in Ref. 14, which gives worse fitting.
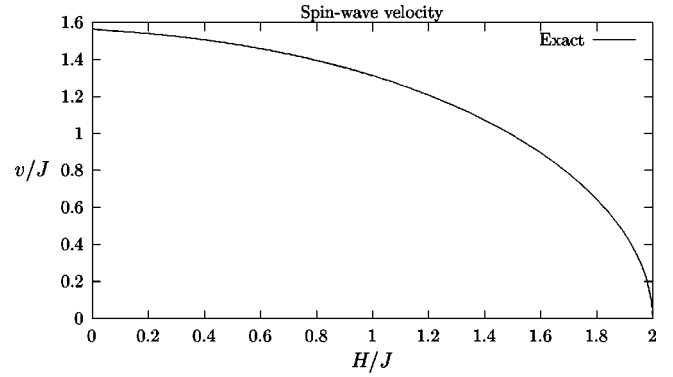

FIG. 9. Spin-wave velocity v as a function of the applied field H, determined from Bethe ansatz integral equations.

which break Lorentz invariance. The net effect is that the H dependence of R becomes more complicated at larger H and also the spin-wave velocity also change with H. We have so far set it equal to 1. It is known to have the value $\pi J/2$ from the Bethe ansatz, for the Heisenberg model at $H=0$. It can be determined numerically from the Bethe ansatz integral equations,[14] and is given in Fig. 9.

Apart from the functions $v(H)$ and $R(H)$, we will also be interested in the behavior of the magnetization, $m(H)$. From bosonization we obtain

$$m(H) \to \frac{H}{2\pi v}, \qquad (4.18)$$

as $H \to 0$. One way of obtaining this result is from calculating the zero field susceptibility:

$$\chi = \frac{1}{T}\left\langle \left(\sum_j S_j^z\right)^2\right\rangle_T = \frac{1}{2\pi T}\left\langle \left(\int dx \frac{\partial \phi}{\partial x}\right)^2\right\rangle_T. \qquad (4.19)$$

Bosonization leads to an exact relation between the three functions $v(H)$, $R(H)$, and $m(H)$. This follows from calculating the susceptibility at arbitrary field, H, using Eq. (4.4) with the corresponding value of $R(H)$:

$$\frac{dm}{dH} \equiv \chi(H) = \frac{1}{(2\pi)^2 R(H)^2 v(H)}. \qquad (4.20)$$

In particular, in the limit of small H this predicts a logarithmic correction to the magnetization:[15]

$$m \to \frac{H}{2\pi v}\left[1 + \frac{1}{2\ln(J/H)}\right]. \qquad (4.21)$$

Equations (4.17), (4.20), and (4.21) are universal. They should remain true for generic half-integer spin isotropic antiferromagnets in the gapless phase. For the particular case of the nearest neighbor $S = \frac{1}{2}$ Heisenberg model we can set $v = \pi J/2$ in Eq. (4.21). Equation (4.20) agrees very well with our numerical solution of the Bethe ansatz equations. (See Figs. 8, 9, and 10.) As far as we know the first (numerical) calculation of these quantities for $0 < H < 2J$ were Ref. 16 for $m(H)$, Refs. 17 and 18 for $R(H)$, and Ref. 19 for $v(H)$. (Numerical calculations in Refs. 18 and 19 were based on the Bethe ansatz integral equations of Ref. 14.)
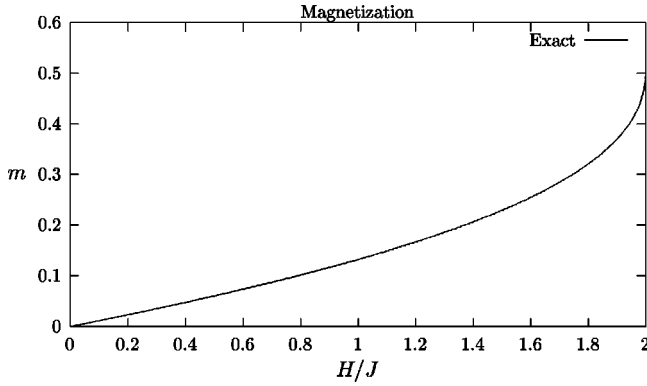
FIG. 10. Magnetization m as a function of the applied field H, determined from Bethe ansatz integral equations.

Once m, v, and R are determined from the Bethe ansatz, all low energy properties of the system are determined by bosonization. From Eq. (4.4) the magnetization can be written

$$m(H) = \frac{1}{2\pi R(H)} \int dx \frac{\partial \phi}{\partial x}. \qquad (4.22)$$

Therefore the exact formula for the field-induced shift in ϕ is

$$\phi \to \phi + 2\pi R(H) m(H) x. \qquad (4.23)$$

All low energy Green's functions are then determined from Eq. (4.4) after shifting $\phi(x)$. In particular we see that G^z has the soft wave vectors 0 and $\pi \pm 2\pi m(H)$ whereas $G^\pm$ has the soft wave vectors $\pm 2\pi m(H)$ and π.

V. BOSONIZATION FOR NONZERO STAGGERED FIELD

Now we consider the effective Hamiltonian of Eq. (2.11) with both uniform and staggered fields nonzero and $h \ll H$. We begin by using the results of the previous section to obtain the $h = 0$ theory with the shifted and rescaled boson field characterized by $R(H)$, $m(H)$, and $v(H)$. For $h = 0$, upon making these transformations, the Lagrangian density is simply the free boson one of Eq. (4.1). From the bosonization formulas of Eq. (4.4) the staggered field adds the interaction term

$$\mathcal{L}_{\text{int}} = hC \cos(2\pi R \tilde{\phi}). \qquad (5.1)$$

Noting the duality transformation between ϕ and $\tilde{\phi}$

$$\partial_t \phi = \partial_x \tilde{\phi}, \quad \partial_x \phi = -\partial_t \tilde{\phi}, \qquad (5.2)$$

we may also write the free Lagrangian in terms of $\tilde{\phi}$:

$$\mathcal{L}_0 = \frac{1}{2}[(\partial_t \tilde{\phi})^2 - (\partial_x \tilde{\phi})^2]. \qquad (5.3)$$

Hence we have the standard sine-Gordon field theory. An impressive array of conjectured exact results are available on this model, which can be brought to bear on the spin-chain problem. The interaction term is sometimes written as $\cos \beta \tilde{\phi}$, so we see that we have $\beta = 2\pi R$. In the next section we will discuss details of the excitation spectrum of this

model. In this section we discuss the dependence of the gap on the uniform and staggered field.

The renormalization group scaling dimension of this operator is πR^2 from which it follows that the gap scales as

$$\frac{\Delta}{J} \to \mathcal{A}\left(\frac{H}{J}\right)\left(\frac{h}{J}\right)^{1/[2 - \pi R(H)^2]}, \qquad (5.4)$$

for some function $\mathcal{A}$. Since, for small uniform fields, $\pi R^2 \approx 1/2$, it follows that the exponent is approximately 2/3, as found in the experiment. Note that this formula is valid for $h \to 0$ at fixed H. This is a reasonable order of limits for describing the experiments since h is only a few percent of H. The exponent is determined by $R(H)$, given in Fig. 8.

We wish to improve on this result in two ways. First of all, if we consider the case where H is strictly 0, then this formula is modified to

$$\Delta/J \to A_0\left(\frac{h}{J}\right)^{2/3} \ln^{1/6}\left(\frac{J}{h}\right). \qquad (5.5)$$

We will calculate exactly the amplitude A_0. This is not of direct relevance to the experiments, however, since they are in the opposite limit $H \gg h$. More importantly, we can determine the amplitude function $\mathcal{A}(H/J)$ in Eq. (5.4) for $H \ll J$:

$$\mathcal{A}\left(\frac{H}{J}\right) \to A \ln^{1/6}\left(\frac{J}{H}\right). \qquad (5.6)$$

We will also determine exactly the numerical factor, A, which is different than A_0 in Eq. (5.5). While the logarithmic factors in Eqs. (5.5) and (5.6) are universal and follow from an RG treatment of the marginal interaction, the exact numerical coefficients are specific to the ordinary nearest neighbor Heisenberg $S = \frac{1}{2}$ model and are obtained by using a remarkable exact conjecture made recently by Lukyanov and Zamalodchikov[7] extended to the Heisenberg point following the method in Ref. 12. (See also Ref. 20.)

Our calculations follow the notation of Refs. 21 and 12. We consider the renormalization group equation obeyed by the effective coupling constant $g(E)$ multiplying the cos interaction in Eq. (5.1), with bare value hC/J for a bare cutoff J, taking into account, to linear order, the effect of the marginal interactions of Eq. (4.9). This is

$$\frac{dg}{d(\ln E)} = -[2 - \gamma(g, \vec{\lambda})]g. \qquad (5.7)$$

The anomalous dimension is given, to low order, by

$$\gamma \approx \frac{1}{2} - \frac{\pi}{\sqrt{3}}\lambda_z. \qquad (5.8)$$

λ_z obeys the RG equation of Eq. (4.10). By the usual scaling arguments, we determined the gap, Δ by reducing the ultraviolet cutoff down to a scale Δ such that $g(\Delta)$ is $O(1)$. Taking into account the dependence of the effective coupling constant, $g(E)$ on the bare coupling constant, h/J, then determines the dependence of the gap on h. In the case $H = 0$, the RG flow of $\lambda_z(E)$ is given by Eq. (4.10) for all E. On the other hand, for finite H, $\lambda_z(E)$ essentially stops renormalizing at a scale of order H. Integrating Eq. (5.7) gives

$$g(E) = \left(\frac{E}{J}\right)^{-3/2} e^{-\pi/\sqrt{3}\int_J^E d\ln E' \lambda_z(E')}. \qquad (5.9)$$

This integral can be conveniently evaluated by changing integration variables to $\lambda_\perp(E')$ using the second of Eqs. (4.10). This gives

$$g(E) \approx g(J)(E/J)^{-3/2}[\lambda_\perp(E)/\lambda_\perp(J)]^{1/4}. \qquad (5.10)$$

Determining the gap by the condition $g(\Delta) = 1$ and setting $g(J) \propto h/J$, gives

$$h/J = B(\Delta/J)^{3/2}[4\pi\lambda_\perp(\Delta)/\sqrt{3}]^{1/4}, \qquad (5.11)$$

for some nonuniversal constant B, of $O(1)$.

In the case $H = 0$, the solution of the RG equation, Eq. (4.10), is

$$\lambda_\perp(\Delta) \approx \frac{\sqrt{3}}{4\pi \ln(J/\Delta)}. \qquad (5.12)$$

Thus,

$$\Delta/J = B^{-2/3}(h/J)^{2/3}[\ln(J/h)]^{1/6}[1 + O(1/\ln(J/h))]. \qquad (5.13)$$

For nonzero H, the first of Eq. (4.10) is only valid for $E \gg H$. At lower energies, λ_z stops renormalizing. Its fixed value at low E determines $R(H)$:

$$2\pi\lambda_z(0)/\sqrt{3} = 1 - 2\pi R(H)^2 \approx \frac{1}{2\ln(J/H)}. \qquad (5.14)$$

We can extend somewhat the accuracy of our results to larger H, by expressing the subsequent results in terms of $R(H)$, determined numerically from the Bethe ansatz, rather than by using the above asymptotic small H result for $R(H)$. For $\Delta \ll H$, we use the second of Eq. (4.10) with λ_z fixed at $\lambda_z(0)$ as given by Eq. (5.14) and the initial condition

$$\lambda_\perp(H) \approx \lambda_z(H) \approx \lambda_z(0), \qquad (5.15)$$

to obtain

$$\lambda_\perp(E) \approx \frac{\sqrt{3}}{2\pi}[1 - 2\pi R(H)^2]\left(\frac{E}{H}\right)^{2[1-2\pi R(H)^2]}. \qquad (5.16)$$

Setting $E = \Delta$ and substituting into Eq. (5.11) gives

$$\frac{h}{J} = B\left(\frac{\Delta}{J}\right)^{2-\pi R^2}\left(\frac{J}{H}\right)^{(1-2\pi R^2)/2}[2(1-2\pi R^2)]^{1/4}. \qquad (5.17)$$

Thus we obtain Eq. (5.4) with

$$\mathcal{A}(H/J) \approx \left\{B\left(\frac{J}{H}\right)^{(1-2\pi R^2)/2}[2(1-2\pi R^2)]^{1/4}\right\}^{-1/(2-\pi R^2)}. \qquad (5.18)$$

Note that in Eq. (5.4) and (5.18), R is a function of H, shown in Fig. 8 and given approximately by Eq. (5.14). As $H \to 0$, we may evaluate $\mathcal{A}(H)$ explicitly, from Eq. (5.14). Using

$$\left(\frac{J}{H}\right)^{1/4\ln(J/H)} = e^{1/4}, \qquad (5.19)$$

this gives

$$\mathcal{A}(H) \to B^{-2/3}e^{-1/6}[\ln(J/H)]^{1/6}. \qquad (5.20)$$

Note that the same numerical constant, B, occurs in the $H = 0$ case, Eq. (5.13) and the $H \gg \Delta$ case, Eqs. (5.4) and (5.20). However, in the latter case it gets multiplied by an extra factor of $e^{-1/6}$.

Finally we wish to determine the dimensionless amplitude, B, appearing in Eq. (5.11) and below. This can be done using two remarkable results. One of them is the exact proportionality constant in the bosonization formula for the staggered part of S_j^x, that is the constant C in Eq. (4.4). This fixes the coupling constant in the sine-Gordon model, Ch, in Eq. (5.1). The other recent result is the exact relationship between the sine-Gordon coupling constant and the mass of the lightest particle in the spectrum of the sine-Gordon model, which is the gap, Δ. This determines the exact relationship between Δ and h. This calculation was done in zero uniform field for the xxz $S = \frac{1}{2}$ antiferromagnet of Eq. (4.5). The calculation was performed for all δ along the critical line, $-1 < \delta < 1$. Due to the logarithmic corrections at the isotropic point, $\delta = 1$, an additional calculation is needed at that point. This can be done using the RG. We essentially just need to apply Eq. (5.11) to the case of $H = 0$ but δ slightly less than 1. Comparing to the exact result for all $\delta < 1$ then determines the coefficient, B.

For $\delta < 1$ and $H = 0$ we use the RG equations of Eq. (4.10) at low energies. The RG flows are hyperbolas terminating on the positive λ_z axis. These flows are conveniently labeled by

$$\epsilon \equiv 4\pi\lambda_z(0)/\sqrt{3} = 2[1 - 2\pi R^2] = 2\frac{\cos^{-1}\delta}{\pi}. \qquad (5.21)$$

The solution of Eq. (4.10) with this initial condition is

$$\frac{4\pi\lambda_\perp(\Delta)}{\sqrt{3}} = \frac{\epsilon}{\sinh[\epsilon \ln(J/\Delta)]}. \qquad (5.22)$$

Substituting into Eq. (5.11) gives

$$\frac{h}{J} \to B\left(\frac{\Delta}{J}\right)^{3/2}\left\{\frac{\epsilon}{\sinh[\epsilon \ln(J/\Delta)]}\right\}^{1/4}. \qquad (5.23)$$

Note that in the isotropic limit, $\epsilon \to 0$, we recover our previous logarithmic result of Eq. (5.5). On the other hand, taking $\Delta/J \to 0$ with ϵ held fixed it gives

$$\frac{h}{J} \to (2\epsilon)^{1/4}B\left(\frac{\Delta}{J}\right)^{3/2+\epsilon/4}. \qquad (5.24)$$

By comparing this to the exact result for arbitrary δ (and hence ϵ) we may extract the value of the amplitude, B.

In Ref. 6 the spin correlation function in the xxz antiferromagnet is shown to have the asymptotic behavior

$$\langle S_0^x S_r^x \rangle \to (-1)^r \frac{C(R)^2}{2} r^{-2\pi R^2}, \qquad (5.25)$$

with an exact expression determined for the amplitude $C(R)^2$. In the isotropic limit, $R \to 1/\sqrt{2\pi}$:

$$\frac{C(R)^2}{2} \to \frac{1}{4\epsilon^{1/2}\pi^{3/2}}. \qquad (5.26)$$

In Ref. 7 the operator $\cos 2\pi R\tilde{\phi}$ is normalized so

$$\langle \cos[2\pi R\tilde{\phi}(0)]\cos[2\pi R\tilde{\phi}(r)]\rangle \to \frac{1}{2}|r|^{-2\pi R^2} \qquad (5.27)$$

(after accounting for a difference in normalization of the free boson Lagrangian by a factor of 8π). This determines the exact proportionality constant in the bosonization formula of Eq. (4.4):

$$S_j^x \approx (-1)^j C(R)\cos[2\pi R\tilde{\phi}]. \qquad (5.28)$$

Hence the coupling constant in the sine-Gordon Lagrangian is precisely $C(R)h$. The exact relationship between this coupling constant and the mass, Δ, of the soliton of the sine-Gordon model is

$$\frac{C(R)h}{2} = \frac{\Delta^{2-\pi R^2}}{v^{1-\pi R^2}} \frac{\Gamma(\pi R^2/2)}{\pi\Gamma(1-\pi R^2/2)}$$

$$\times \left[\frac{\sqrt{\pi}\Gamma\left(\frac{1}{2(1-\pi R^2/2)}\right)}{2\Gamma\left(\frac{\pi R^2}{4-2\pi R^2}\right)} \right]^{2-\pi R^2}. \qquad (5.29)$$

Here we have inserted, by dimensional analysis, the spin-wave velocity v. Taking the isotropic limit on both sides of this equation, using $v = \pi J/2$, gives

$$\frac{h}{2\sqrt{2}\pi^{3/4}\epsilon^{1/4}J} \to \left(\frac{\Delta}{J}\right)^{3/2+\epsilon/4} \frac{\Gamma(1/4)}{2\pi^{3/4}\Gamma(3/4)}\left[\frac{\Gamma(2/3)}{\Gamma(1/6)}\right]^{3/2}. \qquad (5.30)$$

We see that this is equivalent to the RG result of Eq. (5.24) with the amplitude determined to be

$$B = 2^{1/4}\frac{\Gamma(1/4)}{\Gamma(3/4)}\left[\frac{\Gamma(2/3)}{\Gamma(1/6)}\right]^{3/2}. \qquad (5.31)$$

From Eq. (5.13), for $H=0$, the gap behaves as

$$\Delta/J \to A_0(h/J)^{2/3}[\ln(J/h)]^{1/6}, \qquad (5.32)$$

with

$$A_0 = B^{-2/3} = 2^{-1/6}\left[\frac{\Gamma(3/4)}{\Gamma(1/4)}\right]^{2/3}\frac{\Gamma(1/6)}{\Gamma(2/3)} \approx 1.77695. \qquad (5.33)$$

Since we were not aware of the result of Ref. 7 at the time, in Ref. 2 the behavior of the gap with staggered field (for $H=0$) was estimated numerically by extrapolating Lanczos results for lengths up to 22 sites. A very good fit to Eq. (5.32) was obtained with

$$A_0 \approx 1.85. \qquad (5.34)$$

Considering the numerical difficulties related to logarithmic corrections this is remarkably good agreement with the exact result of Eq. (5.33). In the experimentally relevant case, $\Delta \ll H$, the gap behaves as in Eq. (5.4) and, for small H/J, the amplitude is given by Eq. (5.6) with, from Eq. (5.20),

$$A = B^{-2/3}e^{-1/6} \approx 1.50416. \qquad (5.35)$$

Thus our expression for the gap becomes

$$\Delta/J \to 1.50416[\ln(J/H)]^{1/6}(h/J)^{1/[2-\pi R(H)^2]}. \qquad (5.36)$$

For larger H/J, greater accuracy might be obtained by using Eq. (5.18) with B given in Eq. (5.31). That is

$$\Delta/J \to \{0.422169(J/H)^{[1-2\pi R(H)^2]/2}$$

$$\times [2(1-2\pi R(H)^2)]^{1/4}\}^{-1/[2-\pi R(H)^2]}(h/J)^{1/[2-\pi R(H)^2]}, \qquad (5.37)$$

where $R(H)$ is given, from the Bethe ansatz, in Fig. 8. Inserting its asymptotic value at low H,

$$2\pi R(H)^2 \approx 1 - \frac{1}{2\ln(J/H)}, \qquad (5.38)$$

gives back Eq. (5.36). We note that, to actually fit the experimental data, we take $h=cH$ for some constant of proportionality which depends on field direction but is generally of order a few %. Thus the actual scaling of gap with field is not a pure power law.

VI. STRUCTURE FUNCTIONS

For $H=0$ it is convenient to use non-Abelian bosonization, Eq. (4.7), so that the interaction term is written

$$\mathcal{L}_{\text{int}} \propto \text{tr}(g\sigma^x). \qquad (6.1)$$

In this case the model has an SU(2) symmetry. Note that when both uniform and staggered fields vanish and ignoring the marginal operator, the symmetry is actually SU(2)$\times$SU(2):

$$g \to UgV^\dagger. \qquad (6.2)$$

These two independent SU(2)'s act on left and right-movers separately. The ordinary SU(2) symmetry of the spin chain is the diagonal subgroup with $U=V$. This symmetry is broken by the staggered field. However, a different SU(2) subgroup of the original SU(2)$\times$SU(2) survives for which

$$V = \sigma^x U\sigma^x. \qquad (6.3)$$

We may redefine the field g by

$$g \to g\sigma^x \qquad (6.4)$$

in which case the interaction becomes $\text{tr}\, g$, which has the diagonal SU(2) symmetry. In fact, this continuum limit interaction arises from a staggered Heisenberg exchange interaction, as occurs in the spin-Peierls problem. The equivalence of the continuum limit of these two apparently very different problems, is a nontrivial consequence of the chiral symmetry which maps $(-1)^j\vec{S}_j$ into $(-1)^j\vec{S}_j\cdot\vec{S}_{j+1}$.

If we assume that the only effect of the uniform field is to add a term to the Hamiltonian:

$$\delta\mathcal{H} = -\frac{H}{\sqrt{2\pi}}\frac{\partial\phi}{\partial x} = -H(J_L^z + J_R^z), \qquad (6.5)$$

then the uniform field can be removed by the gauge transformation:

$$\phi(x) \rightarrow \phi(x) + \frac{H}{\sqrt{2\pi}}x, \qquad (6.6)$$

or equivalently

$$J_{L,R}^z \rightarrow J_{L,R}^z - \frac{H}{2}. \qquad (6.7)$$

(Here we have set $v=1$.) This transforms the matrix field g as

$$g(x) \rightarrow e^{iHx\sigma^z/2}g(x)e^{iHx\sigma^z/2}. \qquad (6.8)$$

This gauge transformation leaves invariant the staggered field term $\mathrm{tr}\, g\sigma^x$. Thus the exact SU(2) symmetry remains in this approximation. However, additional irrelevant terms in the Hamiltonian in the presence of a uniform field break the exact SU(2) symmetry, as evidenced by the change in the parameter R with field. The SU(2) symmetry is only present for $R = 1/\sqrt{2\pi}$.

The non-Abelian bosonization formula for the staggered part of the spin operators (for $H=0$) is

$$\vec{S}_j \approx (-1)^j C\, \mathrm{tr}\, g\vec{\sigma}. \qquad (6.9)$$

The magnetic field leads to the gauge transformation of Eq. (6.8). The parts of the spin operators with wave-vectors near π thus become

$$S_j^a \approx C\cos(\pi j)\mathrm{tr}\, g\sigma^a \quad (a=x,y),$$

$$S_j^z \approx C\{e^{i(\pi+H)j}\mathrm{tr}\, g(1+\sigma^z)/2 - e^{i(\pi-H)j}\mathrm{tr}\, g(1-\sigma^z)/2\}. \qquad (6.10)$$

Now making the transformation $g \rightarrow g\sigma^x$, this becomes

$$S_j^x \approx C\cos(\pi j)\mathrm{tr}\, g,$$

$$S_j^y \approx iC\cos(\pi j)\mathrm{tr}\, g\sigma^z,$$

$$S_j^z \approx C\{e^{i(\pi+H)j}\mathrm{tr}\, g\sigma^-/2 - e^{i(\pi-H)j}\mathrm{tr}\, g\sigma^+/2\}. \qquad (6.11)$$

In general the spectrum of the sine-Gordon theory consists of the soliton, antisoliton, and breathers (soliton-antisoliton bound states).[22] In the SU(2) symmetric case, the excitation spectrum of the sine-Gordon model with $\beta^2 = 2\pi$ consists of a triplet composed of soliton, antisoliton, and lowest breather and a second breather, heavier by a factor of $\sqrt{3}$. The degeneracy of the triplet is a result of the SU(2) symmetry. Due to the SU(2) symmetry, the three elements of the triplet are produced by the 3 operators $\mathrm{tr}\, g\vec{\sigma}$ with equal intensity, whereas the singlet is produced by the operator $\mathrm{tr}\, g$. Thus setting $H=0$ (but not h) the structure functions G^{yy} and G^{zz} would be equal. Note that, for $H=0$, $S_j^z \propto \mathrm{tr}\, g\sigma^y$, creates the y-polarized member of the triplet. This can be regarded as a

linear combination of the soliton (created by $\mathrm{tr}\, g\sigma^-$) and the antisoliton (created by $\mathrm{tr}\, g\sigma^+$). $G^{zz}(\pi,\omega)$ consists of two identical contributions from the σ^- and σ^+ terms in Eq. (6.11). Each contributes exactly $(1/2)G^{yy}(\pi,\omega)$. The effect of H is to split the soliton and antisoliton contributions to G^{zz} into two separate contributions at different wave vectors $\pi \pm H$. Thus, ignoring the small SU(2) symmetry breaking

$$G^{zz}(\pi\pm H,\omega) = (1/2)G^{yy}(\pi,\omega). \qquad (6.12)$$

It is also interesting to note that the staggered part of the energy density is given by

$$\vec{S}_j \cdot \vec{S}_{j+1} \propto (-1)^j\, \mathrm{tr}\, g. \qquad (6.13)$$

This operator couples to lattice displacements (phonons) and is used to describe Raman scattering experiments. Upon making the gauge transformation of Eq. (6.8) and the redefinition of Eq. (6.4) this becomes

$$\vec{S}_j \cdot \vec{S}_{j+1} \propto e^{i(\pi+H)j}\,\mathrm{tr}\frac{g\sigma^-}{2} + e^{i(\pi-H)j}\,\mathrm{tr}\frac{g\sigma^+}{2}. \qquad (6.14)$$

Thus this operator also creates the soliton and antisoliton. Hence this theory predicts a single particle excitation observable in Raman scattering at the same field-dependent wave vector and frequency as the incommensurate mode observed in neutron scattering.

Upon allowing for SU(2) symmetry breaking the radius changes. After making the gauge transformation, a U(1) symmetry still survives, corresponding to shifting ϕ by a constant. The triplet is now split, with the lowest breather having a different mass than the degenerate soliton antisoliton pair. Since the operators $e^{\pm i\phi/R}$ have charge ± 1 with respect to this U(1) symmetry, we see that the soliton and antisoliton are created by the $q = \pi \pm 2\pi m$ Fourier modes of S_j^z, respectively. The breathers can be classified as even or odd with respect to the discrete symmetry $\tilde{\phi} \rightarrow -\tilde{\phi}$. The odd breathers are created by the $q = \pi$ component of S^y and the even breathers by the $q = \pi$ component of S^x. It can be shown that even and odd breather alternate in the spectrum of the sine-Gordon model. Furthermore, the number of breathers increases with decreasing R. A third breather drops below the soliton antisoliton ($s\bar{s}$) continuum immediately as soon as R decreases below the isotropic value, $1/\sqrt{2\pi}$ with another one dropping below the $s\bar{s}$ continuum each time $2/\pi R^2$ passes through an integer. The mass of the nth breather, expressed in terms of the soliton mass, M, is

$$M_n = 2M\sin(n\pi\xi/2), \qquad (6.15)$$

where

$$\frac{1}{\xi} \equiv \frac{2}{\pi R^2} - 1. \qquad (6.16)$$

Thus the odd-numbered breathers contribute single-particle poles to G^{yy} and the even-numbered ones to G^{xx} while the soliton and antisoliton contribute single-particle poles to G^{zz}. In addition, various multiparticle continua contribute to the three spectral functions.

For a field of 7 T we estimate $\pi R^2 = 0.41$. There are 3 breathers at this point, with masses $0.79M$, $1.45M$, and $1.87M$. A resolution limited peak was observed at $q = 1.22\pi$, at energy 0.22 meV. We identify this with the soliton (or antisoliton) contribution to G^{zz}; hence $M = 0.22$ meV. A resolution limited peak is clearly observable in the neutron scattering data at $q = \pi$ and an energy of 0.17 meV$= 0.77M$. This agrees very well with the prediction for the first breather mass.

We may also test the SU(2) prediction of Eq. (6.12). The SU(2) symmetry is broken by various small effects as exemplified by the fact that $\pi R^2 \neq 1/2$. In particular, this implies that $G^{yy}(\pi, \omega)$ has a second peak, of very low intensity, corresponding to the third breather. Ignoring these effects we expect the intensity of the lowest breather peak in G^{yy} to be approximately twice the intensity of the soliton peak in G^{zz}.

However, before a comparison can be made with experiment it must be taken into account that the unpolarized neutron scattering cross section contains an important direction dependence arising from the Fourier transform of the dipole-dipole interaction between the neutron and the spins. The cross section can be written

$$\sigma(\vec{k}, \omega) = \sum_a (1 - \hat{k}_a^2) G^{aa}(\vec{k}, \omega) f(\vec{k}), \qquad (6.17)$$

where $\hat{k}$ is a unit vector in the direction of $\vec{k}$ and the function $f(\vec{k})$ is slowly varying. Thus the soliton, even breathers and odd breathers are weighted by different factors $1 - \hat{k}_z^2$, $1 - \hat{k}_x^2$, and $1 - \hat{k}_y^2$, respectively. We also have to consider the variation of $f(\vec{k})$ in examining the relative intensity of solitons to breathers since they occur at different values of k_z. It must be recalled that $\hat{x}$ here refers to the direction of the effective staggered magnetic field (and $\hat{z}$ the direction of the uniform field). In the neutron scattering experiments the field was along the b axis. We note that the a'' axis is rotated by about $-17°$ from the crystal axis, a. [We define the rotation angle in the ac ($a''c''$) plane so that c axis is $+90°$ rotated from a axis.]

Strictly speaking, we must take into account the effect of the redefinition of the spin operators, discussed in Sec. II, that was used to eliminate the DM interaction. Letting $\tilde{S}_j^a$ to be the rotated spin operators, defined in Eq. (2.4), and inverting the transformation, we may write the structure function for the original spin operators in terms of the structure function for the rotated operators, which we write as $\tilde{G}^{ab}(k)$. In this way we obtain

$$G^{xx}(k) = \cos^2(\alpha/2)\tilde{G}^{xx}(k) + \sin^2(\alpha/2)\tilde{G}^{yy}(k - \pi),$$

$$G^{yy}(k) = \cos^2(\alpha/2)\tilde{G}^{yy}(k) + \sin^2(\alpha/2)\tilde{G}^{xx}(k - \pi). \qquad (6.18)$$

G^{xy} remains 0 due to translation invariance and the G^{az} are unaffected by the transformation. Here x and y refer to two axes orthogonal to $\vec{D}$ (*not* orthogonal to $\vec{H}$ as in most of this paper.) We expect the second terms in Eqs. (6.18) to be negligible since α is small. Furthermore, the $\tilde{G}^{aa}(k)$ are small for $k \approx 0$ also making the second terms in Eq. (6.18)

smaller than the first for k near π. Henceforth we ignore this small correction and simply use $\tilde{G}^{aa}(k) \approx G^{aa}(k)$.

The direction (and magnitude) of the effective staggered field depends on both the staggered part of the g-tensor and DM interaction. Since the DM interaction in Cu benzoate is unknown, the direction $\hat{x}$ is not known at present. (The DM interaction in Cu benzoate may be estimated from various experimental results based on the present theory. We will discuss this issue in the next section.) However, the direction $\hat{x}$ can be deduced from the polarization analysis[23] of the neutron scattering experiment. Dender *et al.* analyzed the polarization of the neutron scattering at constant energy $\hbar\omega = 0.21$ meV and various momentum transfers. For magnetic field $H = 7T \| b$ and momentum transfer along the chain π, this should probe the lowest ($n = 1$) breather. As discussed above, this odd breather is polarized orthogonal to the total effective staggered field. In Ref. 1 it was claimed that the observed scattering is polarized in the a'' direction. Also note that a misstatement of the crystal orientation occurred in Ref. 23 so that the wrong sign appeared there for $\vec{k} \cdot \vec{a}$.[22] Correcting this error, the polarization is $+18°$ from a axis, or equivalently $+35°$ from a'' axis. This implies that, for an applied field in b direction, the total effective staggered field $-72°$ ($+108°$) from a axis, or equivalently $-55°$ $-55°$ ($+125°$) from a'' axis. (There is actually another feature of the polarization analysis in Ref. 23 which appears inconsistent with the theory presented here, namely the polarization analysis in zero field. The strong dependence of the intensity on the a component of the momentum is taken to indicate that $G^{bb} \approx 0$. Our work ignores any anisotropy in the zero field limit and therefore predicts $G^{bb} = G^{aa} = G^{cc}$ in that limit. We do not understand the source of this discrepancy at present.)

The constant-Q (momentum transfer) scan experiments, sensitive to the breather modes, were carried out at the fixed momentum transfer:

$$(\vec{k} \cdot \vec{a}, \vec{k} \cdot \vec{b}, \vec{k} \cdot \vec{c})/2\pi = (-0.3, 0, 1), \qquad (6.19)$$

where the lattice constants are $a = 6.91A$, $b = 34.12A$, and $c = 89.3A$. Here we have again corrected the misstatement[24] of the crystal orientation in Ref. 1 mentioned above. Note that the antiferromagnetic wave vector, in the chain direction, is actually $2\pi/c$ rather than the normal π/c, because there are two Cu atoms per unit cell along the c axis. The crystal axes a, b, and c are essentially orthogonal. Thus, in the a-b-c system

$$\hat{k} = (-0.26, 0, 0.97), \qquad (6.20)$$

$\hat{k}$ is rotated $+105°$ from the a axis, or $+122°$ from the a'' axis. We note that, this $\hat{k}$ is almost parallel to the direction of the total effective staggered field estimated from the polarization analysis above.

The constant-Q scan for the soliton modes was done for a slightly different momentum transfer

$$(\vec{k} \cdot \vec{a}, \vec{k} \cdot \vec{b}, \vec{k} \cdot \vec{c})/2\pi = (-0.3, 0, 1.12). \qquad (6.21)$$

However, the direction of this momentum transfer $\hat{k}$ is almost the same as the above and we will ignore the difference.

The fact that, an intense first breather peak is observed experimentally, supports the deduction that $\hat{k}$ is nearly parallel to the total effective staggered field. In fact, assuming that $\hat{k}$ is completely parallel to the staggered field, the approximate SU(2) prediction is that the lowest peak at $k = \pi$ (from the first breather in G^{yy}) should have twice the intensity of the lowest peak at $k = \pi \pm H$ (from the soliton/antisoliton in G^{zz}). This prediction is only a very approximate one due to the breaking of SU(2). There could also be corrections from the function $f(\vec{k})$ in Eq. (6.17). Experimentally this ratio appears to be about 2.8. This is perhaps satisfactory agreement. This agreement is only worsened if $\hat{k}$ deviates from the direction of the staggered field.

Thus, analyses of polarization and of the scattering intensity of the lowest breather mode are consistent, and apparently lead to the conclusion that the total staggered field for $H \| b$ is almost parallel to the $\hat{k}$ direction of Eq. (6.20) used in the constant-Q scan.

On the other hand, in Ref. 2 we discussed a feature in the experimental data at $k = \pi$, and $\omega = 0.34$ meV $= 1.55M$. This is very close to the predicted mass of the second breather, which contributes to G^{xx}. A recent calculation, based on integrability of the sine-Gordon model, indicates that the relative intensity of the second breather in peak in G^{xx} should be roughly 1/2 of the intensity of the first breather in G^{yy}. However, we expect this to have essentially zero intensity in the neutron scattering cross section due to the factor of $1 - \hat{k}_x^2$ in Eq. (6.17). [In Ref. 5 an apparently good agreement between theory and experiment was obtained because the factors of $(1 - \hat{k}_a^2)$ were not included. In Ref. 2 intensities were not considered.] A possible resolution of this disagreement is that this ''feature'' at $\omega = 0.34$ meV, discussed by two groups of theorists, is just noise. As stated in Ref. 23, ''Given the quality of the data, this double-gap conjecture is highly speculative.'' Clearly more data is needed to determine whether or not there is really another sharp peak at this frequency. An even more statistically insignificant feature in the data, at $k = \pi$ and $\omega = 0.44$ meV, was discussed in Ref. 5 where it was interpreted as the third breather peak in G^{yy}. Both the energy ($\approx 2M$) and the intensity (very approximately 1/6 the intensity of the first breather) agree with the predictions of the sine-Gordon model. Note that in this case the factor of $1 - \hat{k}_y^2$ is common to first and third breathers so it does not affect the intensity ratio. However, once again, considerably more data is needed to determine if there is really a peak at this frequency.

Another striking feature of the neutron scattering data is a second resolution limited peak at $k = \pi$ and $\omega = 0.8$ meV $\approx H$. This also has a possible interpretation in our field theory approach. It is natural to assume that this peak actually comes from G^{zz}. At this wave vector, from Eq. (6.11), this is proportional to $\langle \mathrm{tr}\, g\, \sigma^{-}\ \mathrm{tr}\, g\, \sigma^{+} \rangle$ at wave vector $k = H$. We expect the continuum limit to hold for some range of wave vectors close to the gap minimum at wave vector $\pi + H$. Thus, at least for weak enough fields, we would expect

the soliton to persist as a single-particle excitation in G^{zz} up to wave vector π. Its energy should obey the Lorentz invariant formula:

$$\omega = \sqrt{M^2 + k^2} = \sqrt{M^2 + H^2}. \quad (6.22)$$

(Here k is measured from the incommensurate wave vector $k + H$ and v is set equal to 1.) Since $H \gg M$ this gives approximately $\omega = H$, as seen in the experiment. The intensity of this feature in G^{zz} can be easily calculated. The result follows from the fact that the k near π parts of the spin operators are all Lorentz scalars. The matrix element between ground state and a single particle excited state of a Lorentz scalar operator is independent of the momentum of the particle, by Lorentz invariance (assuming a Lorentz-invariant normalization of the state). It then follows that the soliton and antisoliton peaks in G^{zz} have an intensity that is proportional to $1/\omega$. The energy is approximately four times higher at $k = \pi$. We must also take into account that both soliton and antisoliton are contributing at $k = \pi$ which increases the intensity by a factor of 2. Thus, we expect the single-particle peak at $\omega \approx H$, $k = \pi$ to have an intensity approximately 1/2 that of the peak at $k = \pi + H$. Experimentally this ratio looks somewhat larger than 1/2 but it must be remembered that the peak at $\omega \approx H$, $k = \pi$ is sitting on top of a background from G^{yy}. Taking this into account, the agreement looks fair.

There is actually a possible objection to this argument. The same reasoning would seem to imply sharp peaks near $\omega = H$ at $k = \pi + H$ coming from G^{yy} and G^{xx}. These were not observed experimentally; at most a small shoulder was observed beginning at $\omega = H$ for $k = \pi + H$. This may simply mean that the breathers have merged into the continuum by this wave vector (due to nonrelativistic effects not contained in the continuum limit field theory), whereas the soliton has not.

We note that spin-wave theory fails to capture the one-dimensional quantum fluctuation dominated physics in various ways. It predicts a single low energy mode with $\Delta \propto h^{1/2}$, instead of $h^{2/3}$ with soft wave vectors π and 0, missing the incommensurate shift. It also predicts another single particle mode at energy approximately H, at the same wave vectors.

VII. ESTIMATE OF DM VECTOR

In the present framework, the only unknown parameters of Cu benzoate are the DM vector, which has not been determined directly in previous studies. Based on the present theory, we can in principle determine the DM vector from several experimental results. Actually, there seem to be no solution that can perfectly fit all the available experimental data, as explained below. Presumably, a precise error estimate on an experiment gives a permissible region for the DM vector, and such constraints from several experiments would give a region of possible values of the true DM vector. However, it should be noted that we have been ignoring the interchain effects, irrelevant operators, etc., which might be necessary in such a precise discussion.

Firstly, as argued in Sec. II, $\vec{D}$ must lie in the a''-c'' plane, leaving two free parameters. The total staggered field is determined by Eq. (2.9).

Here we list the constraints on the DM vector from various experiments.

A. Angular dependence of the gap

As observed in Ref. 1, the induced gap is strongly dependent on the direction of the applied uniform field. In the present theory, this is accounted by the field direction dependent constants of proportionality between the uniform and staggered magnetic fields. As discussed in Sec. II, the proportionality constant should be given by the g tensors and the DM vector $\vec{D}$. Since the g tensors were obtained previously,[9] the measured gap can be used to determine $\vec{D}$.

The gap is proportional to essentially the 2/3 power of this effective staggered field. The specific heat measurements of Ref. 1 were fit by the authors to the specific heat of a collection of free massive relativistic bosons. The masses were found to scale approximately as $H^{2/3}$ with a direction dependent amplitude in the $a'':b:c''=0.55:1.0:2.0$. In Ref. 2, this ratio was used to estimate the DM vector.

Very recently[8] the specific heat of the sine-Gordon model was calculated from the thermal Bethe ansatz and fit to the Cu benzoate data. Again a good fit of the gap to $H^{2/3}$ was obtained for fields in the b or c'' directions with a somewhat different amplitude ratio $b:c''=1.0:2.2$. [The velocity $v(H)$ is another parameter in the fit. This may also be determined from Bethe ansatz for the $S=\frac{1}{2}$ chain in a uniform field. A slightly better fit to the specific heat data was obtained in Ref. 8 by letting $v(H)$ be a free parameter.]

A reasonable fit was not obtained for the field in the a'' direction where the specific heat data is nearly linear. This suggests that, for $H\|a''$ the apparent gap structure was either due to some sort of experimental error or due to other mechanisms[8] than the effective staggered field. In any case, it seems that the effective staggered field for $H\|a''$ is rather close to zero. This implies the cancellation of the effective staggered field coming from the staggered g tensor and the DM interaction. It is not quite unnatural, because for the applied field in ac plane, both the staggered field generated by the staggered g tensor and the DM interaction point to b direction. Thus there is a direction in the ac plane where the cancellation occurs, for a wide range of parameters. Actually, the cancellation of the staggered field is also consistent with the electron spin resonance (ESR) result, which will be explained later.

Assuming the cancellation of the staggered field for $H\|a''$, and that observed gap for $H\|b$ and $H\|c''$ are entirely due to the staggered field, the ratio of the proportionality constants between staggered and uniform fields for $H\|a''$, $H\|b$, and $H\|c''$ are $0:1:(2.2)^{3/2}=3.26$. The ratio gives a constraint on the DM vector through Eq. (2.9).

B. Magnitude of the gap

Based on several exact results on the sine-Gordon field theory and on the $S=\frac{1}{2}$ Heisenberg antiferromagnetic chain, we have determined the magnitude of the gap for a given staggered field h. Thus, comparing this with the gap estimated from the specific heat measurement, we can fix the proportionality constant c between the staggered field h and the applied field H ($h=cH$).

Here we use only the result for $H\|c''$, which is presumably most reliable. For $H\|c''$, the gap is very well fit by the power law $\Delta=kH^{2/3}$, without introducing the logarithmic correction. The proportionality constant is given by $k=1.316$ if Δ and H are measured in units of kelvin and tesla, respectively. By comparing this with Eq. (5.32) and (5.33), where we assume the logarithmic factor to be close to unity for the present case, we obtain $c=0.111$. This also gives a constraint on the DM vector through Eq. (2.9).

C. ESR linewidth

An anomalous broadening of ESR, which is strongly dependent on the field direction, at low temperatures was observed[25] in Cu benzoate. The mechanism of this broadening was left unexplained. However, we have recently developed a field-theory approach to ESR on quantum spin chains at low temperature.[26] According to the theory, the contribution of the staggered field to the ESR linewidth is given by

$$\Gamma \propto \frac{h^2}{T^2}. \tag{7.1}$$

This diverges at lower temperature, in agreement with the experiment. The direction dependence can also be explained by the direction-dependent proportionality constant between the effective staggered field and applied uniform field. Actually, this is consistent with the previous discussion on the field-induced gap, at least qualitatively. In particular, for $H\|a''$, the low-temperature anomalous part of the ESR linewidth vanishes. This implies the cancellation of the staggered field for $H\|a''$. While this appears to contradict the apparent gap found in Ref. 1, it is rather consistent with more refined analysis discussed in the last subsection. In addition, $H\|c''$ gives the largest linewidth, which is consistent with the larger field-induced gap for $H\|c''$.

On the other hand, the ratio of the staggered field is not quantitatively consistent with the specific heat measurement. The estimate of the staggered field is somewhat subtle because there are also contributions to the ESR linewidth from other sources (most importantly exchange anisotropy/dipolar interaction). The low-temperature anomalous part, which is related to staggered field, appears to be approximately 1:4.6 for $H\|b$ and $H\|c''$. This gives the ratio of the staggered field 1:2.1 for $H\|b$ and $H\|c''$. This is smaller than expected from the specific heat analysis.

D. Neutron scattering

As we have discussed in Sec. VI, the analyses on the polarization and intensity of the first breather suggests that the total effective staggered points to $-72°$ ($+108°$) from a axis, or equivalently $-55°$ ($+125°$) from a'' axis, if the external field is applied in b direction. This gives another constraint on the DM vector.

E. Summary of the estimate of the DM vector

There are several experimental data which give some constraints on the DM vector, and they are not perfectly consistent. The estimate of DM vector is also sensitive to the as-
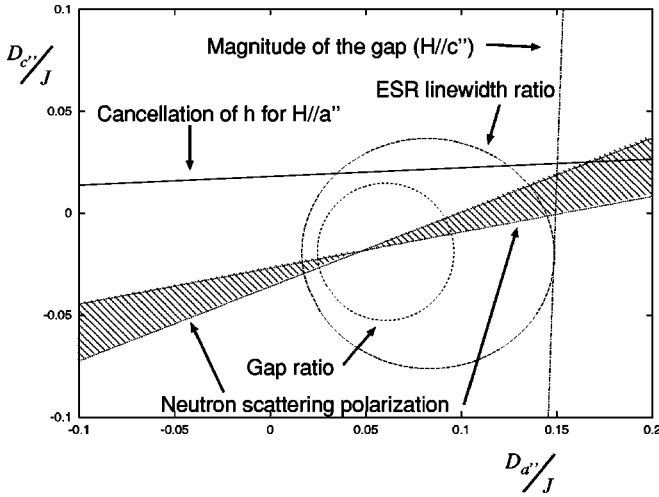
FIG. 11. Estimate of the DM vector from various experiments. Each constraint gives a set of allowed DM vectors as a curve in $D_{a''} - D_{c''}$ plane. The constraint from neutron scattering polarization is drawn with an assumed error of $\pm 5°$.

sumed form of the g tensor, extracted from ESR measurements.[9] The experimental data are presumably subject to several errors which has not been identified precisely. We hope that more experimental data will be available in the future to make more precise comparison with the theory.

The ESR linewidth was measured for various directions of the applied field. Thus it is perhaps quite reliable that the staggered field precisely cancels at $H \| a''$. As we have discussed, this is rather consistent with the refined specific heat result. This gives a single constraint on the DM vector. In the linearized approximation, it reads

$$h_{a''} = 0.0190 + 0.0453 \frac{D_{a''}}{J} - 1.058 \frac{D_{c''}}{J} = 0. \quad (7.2)$$

The estimated ratio of the staggered field for $H \| b$ and $H \| c''$ was inconsistent between the specific heat and ESR. However, it should be recalled that each analysis has its own problem. In the specific heat analysis, an apparent gap structure, which is unrelated to the staggered field, was observed for $H \| a''$. Whatever the origin of this gap structure, it is natural to expect similar contributions also for other field directions. Unfortunately, we do not know how to estimate these effects at present. On the other hand, there are also contributions to the ESR linewidth from other sources than the staggered field, and the subtraction causes some uncertainty, in addition to the estimate of the linewidth itself.

The constraints on the DM vector from various experimental results are summarized in Fig. 11. For the case of neutron scattering polarization we have included an estimated error bar from the polarization analysis of Ref. 23. We have not attempted to estimate error bars in the other cases. We see that a candidate DM vector $(D_{a''}, D_{c''}) \sim (0.13, 0.02)J$, which satisfies the most reliable requirement of the cancellation for $H \| a''$, is roughly consistent with all the constraints except for the ratio of the gap between $H \| b$ and $H \| c''$.

This suggests that the observed ratio of the gap was wrong, or was affected by factors other than the staggered field. More experimental data are needed to draw a reliable conclusion.

VIII. SUSCEPTIBILITY

In the first subsection we consider the staggered susceptibility, resulting from the application of a staggered magnetic field, using the mapping onto the sine-Gordon model. In the next subsection we combine this with the standard uniform magnetization of the $S = \frac{1}{2}$ Heisenberg model to obtain the total physical susceptibility.

A. Staggered susceptibility

We first discuss the susceptibility of the sine-Gordon model. Writing the sine-Gordon Lagrangian in the form

$$\mathcal{L} = \frac{1}{2} \partial_\nu \phi \partial_\nu \phi + 2\mu \cos(\sqrt{2\pi}\phi), \quad (8.1)$$

and adopting units where the velocity is set to 1, we define the sine-Gordon susceptibility as

$$\chi \equiv -\frac{\partial^2 F}{\partial \mu^2}, \quad (8.2)$$

where F is the free energy. The ground state energy (i.e., the $T = 0$ free energy) is expressed in terms of the gap as[27,28]

$$E_0 = -\frac{\Delta^2}{4\sqrt{3}}. \quad (8.3)$$

This determines the $T = 0$ susceptibility using the exact relationship between the coupling constant, μ, and the mass Δ:

$$\Delta = \mu^{2/3} \widetilde{A}, \quad (8.4)$$

where[27,28]

$$\widetilde{A} \equiv A_0 2(2\pi)^{1/6} = 2\pi^{1/6} \left[\frac{\Gamma(3/4)}{\Gamma(1/4)} \right]^{2/3} \left[\frac{\Gamma(1/6)}{\Gamma(2/3)} \right] \approx 4.82764. \quad (8.5)$$

This gives the $T = 0$ susceptibility:

$$\chi(0) = \frac{\widetilde{A}^3}{9\sqrt{3}\Delta}. \quad (8.6)$$

The high-temperature susceptibility is given by

$$\chi \to 4 \int_0^\beta d\tau \int_{-\infty}^\infty dx \langle \cos\sqrt{2\pi}\phi(\tau,x)\cos\sqrt{2\pi}\phi(0,0) \rangle. \quad (8.7)$$

This Green's function is normalized to $1/2r$ (at $T = \tau = 0$). At finite τ and T we have

$$\frac{1}{\sqrt{r^2 + \tau^2}} \to \frac{1}{\frac{\beta}{\pi} \left[\sin\frac{\pi}{\beta}(\tau + ix)\sin\frac{\pi}{\beta}(\tau - ix) \right]^{1/2}}. \quad (8.8)$$

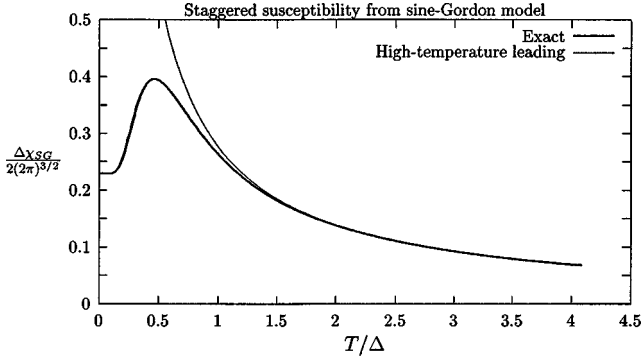Here $\beta \equiv 1/T$. Thus, the susceptibility becomes

FIG. 12. Susceptibility of the sine-Gordon model, as defined by Eqs. (8.1) and (8.2), divided by a factor of $2(2\pi)^{3/2}$. This is essentially the staggered susceptibility of the spin chain, multiplied by Δ, up to a slowly varying logarithmic factor. The exact curve is obtained by a numerical solution of the integral equation, and the high-temperature asymptotics is from the perturbation theory, $0.278\Delta/T$. The $T=0$ value is given by 0.229, in agreement with Eqs. (8.6) and (8.5).

$$\chi(T)\to 2\pi T\int_{-\infty}^{\infty}dx\int_0^{\beta}d\tau\sqrt{\frac{2}{\cosh(2\pi x/\beta)-\cos(2\pi\tau/\beta)}}$$

$$=\frac{1}{T}\left[\frac{\Gamma(1/4)}{\Gamma(3/4)}\right]^2=\frac{8.75376}{T}. \tag{8.9}$$

(This result for the integral can be obtained, by analytic continuation, from the general result of Schulz.[29]) An integral equation determining the sine-Gordon free energy at finite T was given in Ref. 30. We may determine the susceptibility by differentiating twice with respect to μ. Note however that this integral equation actually determines $F(T)-E_0$ so we must add the zero-temperature part of the susceptibility, given above. The resulting susceptibility, $\chi\Delta$ is plotted versus T/Δ in Fig. 12. As expected, it agrees quite well with high temperature result $\sim 8.73576/T$ down to $T\sim\Delta$. It has a maximum at about $T\sim 0.5\Delta$. The $T=0$ value is given by Eqs. (8.6) and (8.5).

Up to a multiplicative factor and logarithmic corrections, the sine-Gordon susceptibility essentially gives the staggered susceptibility of the $S=\frac{1}{2}$ chain, i.e., its response to a staggered field

$$\chi_s(T,h,H)\equiv -\frac{\partial^2 F}{\partial h^2}. \tag{8.10}$$

In order to determine this factor and estimate the logarithmic corrections we first consider the $T=0$ staggered magnetization of the $S=\frac{1}{2}$ chain.

We refer to the staggered magnetization as m_s:

$$\langle S_j^x\rangle=(-1)^j m_s. \tag{8.11}$$

In the continuum limit,

$$m_s\propto\langle\text{tr } g\,\sigma^x\rangle\propto\langle\cos(2\pi R\tilde{\phi})\rangle. \tag{8.12}$$

Since this operator has scaling dimension πR^2, a standard RG scaling argument gives the scaling of the staggered magnetization with staggered field

$$m_s\to\mathcal{D}\left(\frac{H}{J}\right)\left(\frac{h}{J}\right)^{\pi R^2/(2-\pi R^2)} \tag{8.13}$$

for some function $\mathcal{D}$. For weak fields the exponent is approximately 1/3. In a similar way to our analysis of the gap in the previous section, by combining the exact results for the xxz model with an RG analysis of the marginal operator we may determine the scaling of magnetization with staggered field in the case of zero uniform field

$$m_s\to D_0(h/J)^{1/3}\left[\ln\frac{J}{h}\right]^{1/3} \tag{8.14}$$

and determine the behavior of $\mathcal{D}(H/J)$ in Eq. (8.13) for small field

$$\mathcal{D}(H/J)\to D[\ln(J/H)]^{1/3}. \tag{8.15}$$

m_s obeys a standard RG equation relating a change in the cutoff energy scale, E, to a change in the coupling constant, λ:

$$\left[\frac{\partial}{\partial\ln E}-\vec{\beta}(\vec{\lambda})\cdot\frac{\partial}{\partial\vec{\lambda}}-\gamma(\vec{\lambda})\right]m=0. \tag{8.16}$$

Working to linear order in the marginal couplings, as before, we set $\beta\approx 0$ and use Eq. (5.8). Using Eq. (4.10), and lowering the cutoff scale to the gap, Δ, this gives

$$m_s\to F\left(\frac{\Delta}{J}\right)^{1/2}\left[\frac{4\pi}{\sqrt{3}}\lambda_\perp(\Delta)\right]^{-1/4}, \tag{8.17}$$

for some constant, F. Using Eq. (5.11), and Eq. (5.33) this can be written as

$$m_s\to FA_0^{1/2}\left(\frac{h}{J}\right)^{1/3}\left[\frac{4\pi}{\sqrt{3}}\lambda_\perp(\Delta)\right]^{-1/3}, \tag{8.18}$$

where A_0 is defined in Eq. (5.5) and determined in Eq. (5.33). As in the previous sections we obtain the various formulas from the different asymptotic scaling of $\lambda_\perp(\Delta)$ in the three cases: $H=0$, $H\gg\Delta$, and $H=0$ with exchange anisotropy ϵ, defined in Eq. (5.21). Using Eq. (5.12) we obtain Eq. (8.14) with

$$D_0=FA_0^{1/2}. \tag{8.19}$$

Using Eq. (5.16) we obtain Eq. (8.13) with

$$D\left(\frac{H}{J}\right)=D_0[2(1-2\pi R^2)]^{-1/3}\left(\frac{H}{J}\right)^{-2(1-2\pi R^2)/3}. \tag{8.20}$$

Using Eq. (5.14) we obtain Eq. (8.15) with

$$D=D_0 e^{-1/3}. \tag{8.21}$$

Using Eq. (5.22), in the limit $\Delta/J\to 0$, in Eq. (8.17) we obtain an expression for m_s in terms of Δ with exchange anisotropy:

$$m_s\to F(2\epsilon)^{-1/4}(\Delta/J)^{1/2-\epsilon/4}. \tag{8.22}$$

We may determine the constant F, by comparing to the exact result of Ref. 7. From Eq. (5.28)

$$m_s \to C(R)\langle \exp[2\pi i R \tilde{\phi}]\rangle, \qquad (8.23)$$

with the exact formula for $C(R)$ given in Eq. (5.26). This expectation value is given in terms of the soliton mass, Δ in Ref. 7, Eq. (15), with

$$\beta = \sqrt{\frac{\pi}{2}} R \approx \frac{1}{2} - \frac{\epsilon}{8}. \qquad (8.24)$$

Inserting a power of the spin-wave velocity, v by dimensional analysis, and taking the limit of small ϵ, we obtain

$$\langle e^{2\pi i R \tilde{\phi}}\rangle \to \frac{(4/3)\pi\Gamma(3/4)}{16\sin(\pi/3)\Gamma(1/4)}\left(\frac{\Gamma(2/3)\Gamma(5/6)}{4\sqrt{\pi}}\right)^{-3/2}$$
$$\times \left(\frac{\Delta}{v}\right)^{1/2 - \epsilon/4}. \qquad (8.25)$$

This gives a result consistent with Eq. (8.23) and determines the constant, F, to be

$$F = 2^{9/4}\frac{\sqrt{\pi}}{3\sqrt{3}}\frac{\Gamma(3/4)}{\Gamma(1/4)}[\Gamma(2/3)\Gamma(5/6)]^{-3/2} = 2A_0^{3/2}/(3\sqrt{3}\pi), \qquad (8.26)$$

where the constant A_0 is defined in Eq. (5.5) and its value is given in Eq. (5.33). Here we have used the exact identity $\Gamma(1/6)\Gamma(5/6) = 2\pi$. Hence the amplitude of Eq. (8.14) is given by

$$D_0 = FA_0^{1/2} = 2A_0^2/(3\sqrt{3}\pi). \qquad (8.27)$$

We thus obtain the $T=0$ staggered susceptibility of the $S = \frac{1}{2}$ chain by differentiating m_s with respect to h

$$\chi_s(T=0,h) = \frac{2A_0^3}{9\pi\sqrt{3}}\frac{\ln^{1/2}(J/\Delta)}{\Delta}, \qquad (8.28)$$

for $H=0$. Comparing to Eqs. (8.5) and (8.6), we see that

$$\chi_s(T=0,\Delta) = \frac{\ln^{1/2}(J/\Delta)}{2(2\pi)^{3/2}}\chi_{SG}(T=0,\Delta). \qquad (8.29)$$

The susceptibility for $T \gg \Delta$ (and $H=0$) follows from Eqs. (8.8) and (8.9). Here we use the exact result for the $T=0$ correlation function of the $S = \frac{1}{2}$ chain[12]

$$\langle S^x(r)S^x(0)\rangle \to \frac{(\ln r)^{1/2}}{(2\pi)^{3/2}r}. \qquad (8.30)$$

This differs from the correlation function of the sine-Gordon model by a factor of $(\ln r)^{1/2}/2(2\pi)^{3/2}$. [Note the factor of 4 difference in the susceptibilities due to the factor of 2 in the interaction term of the sine-Gordon Lagrangian of Eq. (8.1).] Upon going to finite T and Fourier transforming at zero frequency and wave vector, we expect the logarithmic factor to become $\ln^{1/2}(J/T)$. Thus

$$\chi_s(T \gg \Delta) = \frac{0.277904\ln^{1/2}(J/T)}{T} = \frac{\ln^{1/2}(J/T)}{2(2\pi)^{3/2}}\chi_{SG}(T \gg \Delta). \qquad (8.31)$$

Comparing to Eq. (8.29) suggests the heuristic formula

$$\chi_s(T,\Delta) = \frac{\ln^{1/2}[J/\max(T,\Delta)]}{2(2\pi)^{3/2}}\chi_{SG}(T,\Delta). \qquad (8.32)$$

$\chi_{SG}/[2(2\pi)^{3/2}] \approx \chi_s$ is plotted in Fig. 12.

Including a small uniform field, H, only makes unimportant changes in these formulas. At $T=0$, the power of Δ in Eq. (8.28) changes by a small amount; the argument of the logarithm changes to J/H and the amplitude by a factor of $e^{-1/3}$. For $T \gg \Delta$ we must distinguish two regimes, depending on the relative magnitude of H and T. For $\Delta \ll T \ll H$, the power of T changes. On the other hand, for $\Delta \ll H \ll T$ we expect to obtain Eq. (8.31).

B. Physical susceptibility

Above we considered the staggered susceptibility resulting from (independent) staggered and uniform fields. To make any comparison with experiments we must take into account that the effective staggered field is proportional to the uniform field,

$$h = cH, \qquad (8.33)$$

where the constant of proportionality, c is strongly dependent on field direction. The physical susceptibility is conveniently obtained from its thermodynamic definition

$$\chi = -\frac{d^2F}{dH^2}, \qquad (8.34)$$

where F is the free energy. Writing F as a function of uniform and staggered fields, we must set $h = cH$ before taking the H derivative. We may calculate the free energy in the rotated spin basis of Eq. (2.4), used throughout this paper. Noting that the first derivative of F with respect to H or h gives the uniform magnetization, m_u and staggered magnetization m_s respectively (in the rotated basis), we obtain

$$\chi_{phys} = \frac{\partial m_u}{\partial H} + c^2\frac{\partial m_s}{\partial h} + 2c\frac{\partial m_s}{\partial H}, \qquad (8.35)$$

where we have used

$$\frac{\partial m_u}{\partial h} = \frac{\partial m_s}{\partial H} = \int_0^\beta d\tau\langle m_s(\tau)m_u(\tau)\rangle. \qquad (8.36)$$

We may ignore the dependence on h of the first term and use the standard result for the uniform susceptibility of the $S = \frac{1}{2}$ chain, χ_u^0. For low fields and temperatures this gives

$$\frac{\partial m_u}{\partial H} \approx \chi_u^0 \to \frac{1}{2\pi v_s} = \frac{1}{\pi^2 J}, \qquad (8.37)$$

independent of field and temperature. The second term in Eq. (8.35) is larger than the third so we approximate

$$\chi_{phys} \approx \chi_u^0 + c^2\chi_s(h,T), \qquad (8.38)$$

where χ_s is the staggered susceptibility discussed in the previous subsection. Thus, when measuring the physical susceptibility of the present system, one actually probes also the staggered susceptibility.[31]

While the first term, the standard result for the susceptibility of the $S = \frac{1}{2}$ chain, goes to a finite constant, at T and $H \to 0$, the second term, resulting from the effective stag-

gered field, is highly singular. At zero field it blows up at $T \to 0$ as $0.278 \ln^{1/2}(J/T)/T$. Thus, although it is multiplied by the small constant, c^2, it eventually dominates for low enough T. For any finite field, the divergence of the second term is cut off, at essentially the gap energy, $\Delta(h)$, at a value of approximately $0.229 \ln^{1/2}(J/\Delta)/\Delta$, as shown in Fig. 12. At low fields the behavior looks quite similar to a paramagnetic impurity contribution. It can be distinguished from that, however, by its very strong field-direction dependence. The effect is largest for the field in the c direction when the parameter $c^2 \approx 0.01$.

The experimental susceptibility[32] of Cu benzoate shows very peculiar behavior at low fields and temperatures. As the temperature is lowered, in low fields, the susceptibility grows. This effect is highly direction dependent with the biggest effect occurring for fields in the c direction. This effect is cut off by the application of a field. Qualitatively, the experimental results look similar to our predictions. However, at a more quantitative level there are many differences. The anomalous low field low T part of χ is much larger in the experiments than in the theory. For instance, at zero field, a temperature of 1 K$\approx J/18$, and $c^2 = 0.01$, the value that we find for $H \| c$, the second term in Eq. (8.35) is still smaller than the first by a factor of about 1/2. The anomalous contribution could be somewhat larger due to the third term in Eq. (8.35) and the logarithmic correction. However, the anomalous term in χ^c observed in Cu benzoate at this zero field and low T is about six times *larger* than the χ_u^0. This is perhaps too large to be explained by our theory which is purely one-dimensional.

Furthermore, the detailed experimental dependence on T and H is quite complex. The maximum susceptibility occurs at a field of about 30 G and $T = 1.5$ K. At lower fields or temperatures the susceptibility decreases somewhat. At low fields, two extra low temperature peaks are observed in the susceptibility as a function of T (in addition to the normal one for an $S = \frac{1}{2}$ chain at $T \approx 0.6J$). While it is tempting to try to identify the higher-T peak with the peak in χ_s shown in Fig. 12, and the lower-T peak with the onset of Néel order, both susceptibility peaks are broad, unlike what would be expected from a phase transition. (Indeed, no evidence for magnetic order was found from neutron scattering,[23] down to $T = 0.8$ K.) A strong frequency dependence of the low T and H susceptibility was also observed.

We expect that a proper theoretical description of the low field and temperature susceptibility of Cu benzoate will require the inclusion of interchain coupling effects. The interchain superexchange paths look complicated and it is not even clear what is the sign of the interchain coupling. We remark that a perfectly one-dimensional $S = \frac{1}{2}$ antiferromagnet with SU(2) symmetry broken only by the DM interaction has a disordered ground state. This follows from our spin
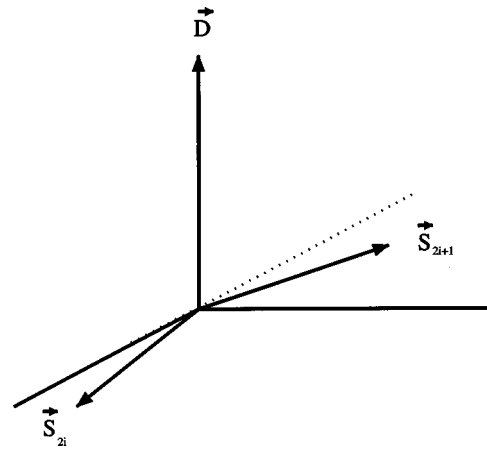

FIG. 13. Spin order for antiferromagnet with DM interaction.

redefinition in Sec. II which maps the system into an *easy plane xxz* model which is well known to have a disordered ground state with power-law correlations. We may think of the spins as fluctuating primarily in the plane perpendicular to $\vec{D}$ with a tendency for the cross product of neighboring spins to be parallel to $\vec{D}$. This system has a U(1) symmetry. Interchain coupling would normally be expected to produce long-range order with both an antiferromagnetic component and a possible perpendicular ferromagnetic component. For example, for $\vec{D} \propto \hat{z}$,

$$\langle \vec{S}_j \rangle = -m_s(-1)^j \hat{x} + m_u \hat{y}. \tag{8.39}$$

(See Fig. 13.)

The standard mean field treatment of the interchain interactions[33] would suggest a critical temperature of order the interchain coupling (assuming that it is antiferromagnetic). On the other hand, when a magnetic field is applied (not parallel to $\vec{D}$), the U(1) symmetry is broken and the phase transition should disappear. m_s and m_u now becomes nonzero even in the purely one-dimensional system and are no longer order parameters for spontaneous symmetry breaking. Thus the application of a magnetic field smoothes out the phase transition in this system. Surprisingly, neutron scattering experiments in zero field have failed to detect a Néel transition.

[1] D. C. Dender, P. R. Hammar, D. H. Reich, C. Broholm, and G. Aeppli, Phys. Rev. Lett. **79**, 1750 (1997).

[2] M. Oshikawa and I. Affleck, Phys. Rev. Lett. **79**, 2883 (1997).

[3] I. Dzyaloshinskii, J. Phys. Chem. Solids **4**, 241 (1958).

[4] T. Moriya, Phys. Rev. **120**, 91 (1960).

[5] F. H. L. Essler and A. M. Tsvelik, Phys. Rev. B **57**, 10592 (1998).

[6] F. C. Alcaraz and A. L. Malvezzi, J. Phys. A **28**, 1521 (1995).

[7] S. Lukyanov and A. Zamalodchikov, Nucl. Phys. B **493**, 571 (1997).

[8] F. H. L. Essler, Phys. Rev. B **59**, 14 376 (1999).

[9] K. Oshima, K. Okuda, and M. Date, J. Phys. Soc. Jpn. **44**, 757 (1978).

[10] L. Shekhtman, O. Entin-Wohlman, and A. Aharony, Phys. Rev. Lett. **69**, 836 (1992).

[11] T. Sakai and H. Shiba, J. Phys. Soc. Jpn. **63**, 867 (1994).

[12] I. Affleck, J. Phys. A **31**, 4573 (1998).

[13] J. L. Cardy, *Scaling and Renormalization in Statistical Physics* (Cambridge University Press, Cambridge, England, 1996).

[14] N. M. Bogoliubov, A. G. Izergin, and V. E. Korepin, Nucl. Phys. B **275**, 687 (1986); V. E. Korepin, N. M. Bogoliubov, and A. G. Izergin, *Quantum Inverse Scattering Method and Correlation Functions* (Cambridge University Press, Cambridge, England, 1993).

[15] M. Karbach and K.-H. Mütter, J. Phys. A **28**, 4469 (1995).

[16] R. B. Griffiths, Phys. Rev. **133**, A768 (1964).

[17] A. Fledderjohann, C. Gerhardt, K. H. Mütter, A. Schmitt, and M. Karbach, Phys. Rev. B **54**, 7168 (1996).

[18] D. C. Cabra, A. Honecker, and P. Pujol, Phys. Rev. B **58**, 6241 (1998).

[19] P. R. Hammar, M. B. Stone, D. H. Reich, P. J. Gibson, M. M. Turnbull, C. P. Landee, and M. Oshikawa, Phys. Rev. B **59**, 1008 (1999).

[20] S. Lukyanov, Nucl. Phys. B **522**, 533 (1998).

[21] I. Affleck, D. Gepner, H. J. Schulz, and T. Ziman, J. Phys. A **22**, 511 (1989).

[22] R. Dashen, B. Hasslacher, and A. Neveu, Phys. Rev. D **11**, 3424 (1975).

[23] D. C. Dender, Ph.D. thesis, Johns Hopkins University, 1998.

[24] D. Reich (private communication).

[25] K. Okuda, H. Hata, and M. Date, J. Phys. Soc. Jpn. **33**, 1574 (1972).

[26] M. Oshikawa and I. Affleck, Phys. Rev. Lett. **82**, 5136 (1999).

[27] R. J. Baxter, *Exactly Solved Models in Statistical Mechanics* (Academic, London, 1982).

[28] C. Destri and H. de Vega, Nucl. Phys. B **358**, 251 (1991).

[29] H. J. Schulz, Phys. Rev. B **34**, 6372 (1986).

[30] M. Fowler and X. Zotos, Phys. Rev. B **25**, 5806 (1982).

[31] M. Matsuura and Y. Ajiro, J. Phys. Soc. Jpn. **41**, 44 (1976).

[32] D. C. Dender, D. Davidović, D. H. Reich, and C. Broholm, Phys. Rev. B **53**, 2583 (1996).

[33] See for example, I. Affleck, M. Gelfand, and R. Singh, J. Phys. A **27**, 7313 (1994); I. Affleck and B. Halperin, *ibid.* **29**, 2627 (1996).